PROJECT FINAL REPORT

Grant Agreement number: 288263
Project acronym: NANO-VISTA

Project title: ADVANCED PHOTONIC ANTENNA TOOLS FOR BIOSENSING AND CELLULAR

NANOIMAGING

Funding Scheme: FP7

Period covered: from: 01/11/2011 to: 31/10/2016

Name of the scientific representative of the project's co-ordinator¹, Title and Organisation:

Prof. Maria F. Garcia-Parajo, ICFO-Institute of Photonic Sciences

Tel: +34 93 5534158 Fax: +34 935534000

E-mail: maria.garcia-parajo@icfo.es

Project website Error! Bookmark not defined. address: www.nanovista.eu



¹ Usually the contact person of the coordinator as specified in Art. 8.1. of the Grant Agreement.

1. Final publishable summary report

1.1 Executive summary

One of the ultimate challenges in biology is to understand the relationship between the structure, function and dynamic of biomolecules in their natural environment: the living cell. Although modern molecular biology has made enormous progress in identifying different cell components, both inside and at the cell surface, observing molecular processes in living cells is still a major goal. Key multimolecular interactions that dictate cell functionality occur at the nanometre scale, a size regime not accessible by classical optical techniques owing to the diffraction limit of light. Also, the molecular concentrations found in living cells or cell membranes are often quite large, typically in the micro- to milli-molar range. As a consequence, to be able to investigate processes between individual units, the excitation and detection volume must be reduced by at least three orders of magnitude compared to confocal volumes. Clearly, knowledge generation in the fields of molecular and cellular biology crucially depends on the development of photonic tools that combine ultrasensitive measurements of protein interactions on living cells with cutting edge microscopic approaches.

The goal of NANO-VISTA is to exploit novel concepts of photonic antennas to develop a new generation of bionanophotonic tools for ultrasensitive detection, nanoimaging and nanospectroscopy of biomolecules, both *in-vitro* and in *living cells*. By taking advantage of the extraordinary field enhancement, directionality and nanofocusing of photonic antennas, our approach will allow single biomolecule detection in ultra-reduced detection volumes, including living cells.

The main objectives of NANO-VISTA are three-fold:

First, to pioneer the technological development of novel photonic antenna geometries (probes & 2D arrays) with improved physical properties that will provide both ultrasensitive detection at high sample concentrations in fluids and *simultaneous* spatial nanometric resolution and sub-ms time resolution in living cells.

Second, to develop high-throughput large-scale nanofabrication of photonic antenna arrays fully compatible with biomolecule detection and live cell nanoimaging while ensuring low cost, improved performance, substrate and design flexibility, and reusability.

Third, to demonstrate the improved performance and functionality of the bionanophotonic technology for *a*) ultra-sensitive detection of biomolecules for diagnostic purposes with transferability into a potential market product and *b*) nanoimaging and nanospectroscopy on living cells being fundamental in strategic applications of cell biology and immunology.

To reach the main objectives, we have implemented six dedicated work packages (WP) to RTD activities, each of them containing **specific objectives** and clear milestones, lead by different expert members of the consortium. Moreover, NANO-VISTA implements one additional WP devoted to dissemination and exploitation plans and a last WP devoted to Management activities.

As a whole, NANO-VISTA is fully targeted to the development of disruptive photonic technologies fundamental in strategic applications such as medicine and biology. To maximise the chances of success we have chosen for an interdisciplinary, trans-national and multi-institutional partnership (including a SME and a Medical Centre). True European specialists, with long standing expertise in the fields of nanophotonics, photonic antennas, large-scale nanofabrication approaches and nanoimmunologists are concentrated in this project strengthening European research cohesion. In the mid-long term we expect that both, cell biologists as well as industrial sectors (biophotonic, microscopy and biotechnology enterprises) will benefit from this new technology.

1.2 Summary description of project context and objectives

Advances in the fields of molecular and cell biology are strongly coupled to the implementation of photonic tools that allow highly-sensitive measurements in living cells at high molecular concentrations and at the nanometre scale. Advances in the last eight-to-ten years in the field of nanophotonics promise to take a leap forward towards truly nanometric optical resolution and have the potential to become key techniques in modern biology by providing tools for studying processes in vitro and in vivo at relevant spatial scales and physiological concentrations. Along these lines, photonic antennas are in principle ideal candidates for nanobioimaging and ultrasensitive biosensing having exquisite lateral and axial resolution and possibility for detecting dynamic events. Photonic antennas exploit the unique optical properties of metallic nanostructures to route and manipulate light at the nanometre scale, converting optical radiation into intense, engineered, localised field distributions. By squeezing light into subwavelength volumes, these nanostructures can efficiently mediate interactions between propagating radiation and nanoscale objects.

Because of these exciting properties, it is believed that future potential applications of photonic antennas will impact many different fields in Science including nano-optical signal processing, sensing and imaging. Yet, efforts beyond the proof-of-principle towards real applications have been scare so far. For this to occur considerable technological challenges have first to be overcome and new/more powerful concepts will still have to be proven and implemented. The project NANO-VISTA has aimed at technology developments driven by progress in nanophotonics with a clear, focussed objective of bringing photonic antennas from the research Lab to true applications in the field of Life Sciences. As such, the major goal of NANO-VISTA has been to exploit novel concepts of photonic antennas to develop a new generation of bionanophotonic tools for ultrasensitive detection, nanoimaging and nanospectroscopy of biomolecules, both in-vitro and in living cells. To reach these goals we have defined three main objectives, which are described below together with a short summary of the major efforts and results obtained during the project.

The *first objective* of the project has been to pioneer the technological development of novel photonic antenna geometries (probes & 2D arrays) with improved physical properties that would provide both ultrasensitive detection at high sample concentrations in fluids and *simultaneous* spatial nanometric resolution and sub-ms time resolution in living cells.

During the course of the project, we have concentrated on the following main tasks: In terms of antenna probes we have focussed on multiple designs of increasing complexity: dipole antennas, gap-dipole antennas, bowtie nano-apertures (BNA), monopole antennas on BNA, nanostar antennas and asymmetric gap antennas. Performance criteria of all such antennas are: strong field enhancement; strong spatial field confinement; polarization control; and emission control (quantum efficiency, lifetime, and directionality). Extensive FDTD simulations have been performed to define the best geometries that provide simultaneously significant field enhancement, confinement at the nanometre scale and either resonant or broadband response for biological applications. Different antenna configurations have been fabricated at the end-face of Al-coated tapered fibres to allow optimal spatial field confinement and applications in the visible (500-700nm). The antennas have been fabricated by FIB-milling (at ICFO NanoPhotonic Laboratories). The general fabrication method involves tapering of the optical fibres, Al deposition of the tapered region, FIB milling to define apertures with sizes close to the wavelength cut-off region (typically between 550nm-700nm) and sequential steps of FIBing to define the final antenna geometry. Reproducibility of the entire fabrication procedure is as high as 70%. In the case of nanostars antennas, we have explored several colloidal synthesis routes to produce ultra-sharp features and select nanostars by single-particle-darkfield micro-spectroscopy or in-situ functionalization to a tapered glass probes in a scanning-probe head on the same microscope.

We have characterised the optical performance of these antenna probes by scanning the antennas in close proximity to fluorescence beads (20 nm in size) and to individual molecules embedded in thin polymer layers. In the case of dipole antennas we obtain resonance response at 170 nm dipole length and \sim 15 x enhancement. In the case of BNA probes, we clearly observed fluorescence features that correspond to individual molecules excited by the antenna. The spatial confinement obtained is \sim 70nm with an enhancement of the optical signal of \sim 6 x. Importantly, our entire probe design allowed \sim 10³ x total improvement in throughput over conventional subwavelength NSOM probes of similar opening area. In the case of monopole on BNA antenna probes, also named hybrid antennas, we have demonstrated dual-colour single molecule nano-imaging with 20nm resolution in both colours and unprecedented localization accuracy in the angstrom range. We have also implemented a new multi-colour parallel excitation scheme with single channel detection and have validated our hybrid antennas for nano-imaging of cell surface receptors on intact cells.

In terms of 2D antenna arrays we have focussed on the fabrication of different geometries that allow the generation of illumination hotspots free of background contribution from far field excitation, which is imperatively necessary for the goals of NANO-VISTA, i.e., single molecule fluorescence correlation spectroscopy in living cells. We have explored biocompatible designs that allow us to beam-up the fluorescence so that low objective lenses would be sufficient for single molecule detection, as well as have taken advantage of the polarization properties of antennas to increase applicability. The main geometries investigated are: a) connected-hole (CH) aperture on gold flakes; b) gold dimer antennas embedded inside gold nano-boxes, c) BNA arrays on Al-coated glass substrates and; d) hybrid antennas; e) Al-dimer antennas on Al-nano-boxes for broadband operation; f) planarised dimer antennas on nano-boxes for live cell research. In the case of CH apertures, they consist of a central zone with two sharp tips facing a nanogap. Fabrication of CH apertures using FIB-milling resulted more successful when using flakes of mono-crystalline gold. In the case of the dimer nano-antennas on boxes, we used FIB technology to fabricate them either in gold to achieve very strong resonance (and thus enhancement) in the red, or Al so that we obtain broadband response (at the expense of lower but still significant field enhancement). Despite the lower enhancement, these structures are extremely interesting for multi-colour experiments in-vitro or in living cells. We also succeeded on the fabrication of BNA antennas carved using FIB on Al-layers deposited on glass coverslips. The characterization of both dimers on boxes and BNA antennas has been performed with fluorescent molecules in solution, using fluorescence correlation spectroscopy. The best working designs have been transferred to the EPFL partner for the fabrication of large antenna arrays (Objective 2). Finally, we have invested efforts on exploiting the directionality properties of antennas. We focussed on arrays of Yagi-Uda antennas, demonstrating their directivity. We have also conceived designs aimed at extended their operation bandwidth (more narrow than absorption bands) and have addressed the challenge of critical nanopositioning of emitters. Specifically, we explored designs beyond the basic interference between dipole elements, looking for directional light emission based on the interference between different multipolar moments, and excited in a single metal antenna element.

The *second objective* of the project has been to develop high-throughput large-scale nanofabrication of photonic antenna arrays fully compatible with biomolecule detection and live cell nanoimaging while ensuring low cost, improved performance, substrate and design flexibility, and reusability.

From the beginning of the project we have explored and optimized several fabrication techniques to fulfil design and substrate flexibility requirements. One of the methods is *direct metal nanocutting*, which has been investigated as a single step process for the fabrication of sub 100nm multilayer plasmonic structures on parylene-c substrates. The second method explored is nano-patterning by *stencil lithography*. Although this method is cost-effective for the fabrication of metallic nanostructures down to 20nm in size, it suffers from blurring, i.e., the lack of definition of sharp nano-features due to the existence of a gap between the stencil and the substrate. Within the project

we have applied compliant and collimated stencil methods to successfully reduce the blurring effects. Moreover, we optimized the reactive ion etching process through nanostencils for the cost-efficient and scalable fabrication of BNA antennas in aluminium. After transferring the BNA structures from the stencil into a SiO_2 hard mask, a subsequent stencil-less RIE step allowed the transfer of BNAs in aluminium thin films with gap widths down to 20 nm.

One of the major obstacles when working with living cells is that the cell surface is rather soft and conformal to its environment. Optical antennas can therefore influence the membrane geometry inducing unwanted curvature and possibly affect the diffusion of membrane components. To overcome these limitations we have developed a process allowing for the fabrication of antennas that would induce no deformation of the cell membrane while providing accessibility of the highest region of field confinement. Following the same large-scale requirements as for the development of the etching through stencil process we investigated a novel lift-off procedure based negative electron beam resists enabling throughputs orders of magnitude higher than typically achieved via FIB along with higher resolution. The control of electron beam lithography and gold evaporation at low temperatures allowed the fabrication of dimers-in-a-box antennas with gaps in the order of 10 nm. Upon lift-off of the metal layer, the antennas are stripped from the substrate with a UV curable polymer in order to obtain a flat surface and to position the narrow gap region at the surface. Finally, we investigated capillary assembly of colloidal nanoparticles as an alternative for the fabrication of high-quality single crystal metal structures with gaps tuneable down to the single nanometre level for strongly coupled plasmonic system.

The *third objective* of the project is to demonstrate the improved performance and functionality of the bionanophotonic technology for *a*) ultra-sensitive detection of biomolecules for diagnostic purposes with transferability into a potential market product and *b*) nanoimaging and nanospectroscopy on living cells being fundamental in strategic applications of cell biology and immunology.

In terms of ultra-sensitive detection of biomolecules for diagnostic purposes, we have followed two different approaches. First, we have demonstrated single biomolecule detection in solution (dyes, DNA strands of different sizes, and proteins) at micromolar concentration conditions by means of dimer-antennas embedded in nano-boxes, and more recently, by in-plane flat surface antennas as described above. By using these approaches we have obtained volume reductions as high as 1700 as compared to confocal excitation, together with fluorescent enhancement factors of 10⁴ to 10⁵. These results demonstrated the possibility for ultra-sensitive detection down to the single molecule level at concentrations that are otherwise inaccessible to diffraction-limited conditions. We also applied this approach to control the degree of fluorescence resonance energy transfer (FRET) on individual DNA constructs containing donors and acceptors dyes, achieving FRET enhancement over distances above 10nm. Moreover, we demonstrated that antennas could be also exploited for detecting FRET on perpendicularly oriented donor and acceptor pairs. Second, together with SME COSINGO we have developed a compact, robust and highly sensitive instrument for biosensing and nanospectroscopy on living cells. In here we have a) developed of a lab-on-a-chip based on 2D nano-antennas and microfluidics and b) developed and tested a stand-alone instrument to perform fluorescence correlation spectroscopy (FCS).

Along the lines of *nano-imaging and nano-spectroscopy* we have explored two approaches. *First*, we have exploited our newly designed multi-colour parallel excitation scheme to simultaneously image different receptors on intact cell membranes using monopole-on-BNA antenna probes, obtaining a spatial resolution of 40nm. Moreover, we have used BNA antenna on probes to record the diffusion of individual lipids on the plasma membrane of living CHO cells. BNA probes are maintained in close proximity to the living cell membrane using a very stable feedback loop that keep the antenna ~10nm above the cell surface during the measurement time (typically 30s). Importantly, we have

been able to collect fluorescence bursts from individual labelled lipids diffusing freely on the cell membrane over spatial dimensions smaller than 50nm. Moreover, we took advantage of the polarization sensitivity of the BNA probes to tune the effective illumination volume. We also extended the application of BNA probes for recording nanoscale multi-colour FCS and FCCS on living cells, which is a major breakthrough in the field. We have demonstrated the feasibility of FCCS using BNA antennas by recording the diffusion of protein receptors on the cell membrane, observing the occurrence of dynamic interactions between individual receptors. Second, we have explored the applicability of large 2D arrays of BNA antennas and planarised-dimers on boxes to record the diffusion of individual biomolecules in vitro, lipids on multi-component lipid bilayers and lipids on living cells seeded on these antenna substrates. We have succeeded to record the diffusion of individual lipids on regions as small as 10nm and have established a direct relationship between the gap size of the antenna (so called FCS-diffusion laws), degree of field enhancement and fluorescence burst duration. From the biological side, our results have revealed nanoscopic cholesterol-enriched fluctuations on multi-component lipid bilayers and have confirmed the existence of nanoscale domains on cell membranes, which are sensitive to cholesterol. Moreover, we have developed optimized protocols for efficient transfection of immune cells, including both cell lines and primary cells, and protocols to manipulate the cellular nano-environment, including the amount of lipids, cholesterol, the actin cytoskeleton and tubulin. Using these approaches we have revealed the role of the lipid environment on the spatiotemporal organization of the integrin receptor LFA-1 on immune cells and its implication for LFA-1 adhesive function.

Based on the results obtained, we consider that NANO-VISTA has been an extremely successful multi-disciplinary project that has crucially benefited from the strong collaboration and integration of the different European partners, including academia and industry. In terms of scientific and technical results, NANO-VISTA has fully accomplished the objectives set up at the starting of the project. Indeed, we have made a leap forward in terms of technology development by bringing photonic antennas into the realm of biophotonic applications. This has been achieved by designing and engineering photonic antennas having the best optical performance, in terms of field enhancement spatial confinement and broadband response. We have then developed appropriate nano- and microfabrication routes to render these devices fully compatible with Life Science applications by maintaining their unique optical properties, while at the same time aiming for large-scale throughput fabrication, reproducibility and low cost. To demonstrate the outstanding performance of the designed photonic antenna devices in different biophotonic applications, we have applied them for in-vitro detection of individual fluorescence molecules, single DNA strands of different lengths and proteins in solution at physiological concentrations (in the micro-molar range), which is at least three-orders of magnitude larger than state-of-art confocal detection. Moreover, we have demonstrated dual colour nano-imaging of individual molecules and individual receptors on intact cell membranes with optical resolutions around 20nm. Finally, we have applied these nanostructure devices to resolve for the first time cholesterol-induced nanoscopic fluctuations on multi-component lipid bilayers and demonstrated the role of cholesterol maintaining nanoscale lipid domains in living cell membranes.

In terms of tangible results of the project, the partners of NANO-VISTA have carried out over 270 dissemination activities directly related (and with appropriate acknowledge) to the project in scientific media including scientific peer-review papers published in high impact journals (42), oral contributions and poster presentations (212, from which 132 correspond to invited talks from the PIs involved in the consortium), as well as eight PhD thesis and three Master thesis. We have established contacts with several companies interested in our technology (WITec and PicoQuant) and have filed two different patents and a third one is currently under evaluation. As a whole, NANO-VISTA has pioneered a new research field in biophotonics and has opened-up new frontiers in the field of bionanophotonics and plasmonics for biosensing and bioi-nanoimaging.

1.3 Description of the main S&T results/foregrounds

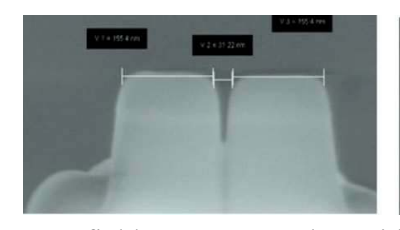
To reach the main objectives of NANO-VISTA we have implemented six dedicated work packages (WP) to RTD activities, each of them containing specific objectives and clear milestones, lead by different expert members of the consortium. Below we describe the main S&T results associated with each WP.

Workpackage 1: Development of photonic antenna probes for nanoimaging and nanospectroscopy on living cells.

As stated in the original granted proposal, WP1 addresses the fabrication and proof-of-principle of scanning antenna probes suitable for nanoimaging and nanospectroscopy of biological samples. The main objectives of this WP were defined as: 1) To explore novel routes of scanning antenna probe geometries to optimise the following physical properties: electric field enhancement, nanofocussing, resonance tuneability and field directionality; 2) Performing dedicated finite difference time domain (FDTD) calculations to serve as guidelines towards the optimisation of antenna geometries; 3) Experimentally measuring the optical properties of antenna probes by using them as nanoimaging tools on individual emitters.

Results associated to novel routes of scanning antenna probe geometries.

In general, the main objective has been to realize free-standing optical antenna probes for local excitation and nanoimaging. One of the first successful designs implemented has been the dipole antenna. These *dipole rod-antennas* have been fabricated in Al for optimal spatial field confinement and applications in the visible (500-700nm). Al antennas have been fabricated by FIB-milling on Alcoated tapered fibres. For actual scanning applications and free access to the sample surface most of the surrounding fibre material is FIBbed away. The most optimised designed turned out to be the gap-dipole antenna (Fig. 1), which consists on a double dipole, separated by a narrow gap. The gap was fabricated by FIB-milling, typically most narrow at the pedestal while wider towards the top area. Smallest gaps of 25-30nm were fabricated, as shown in Fig. 1.



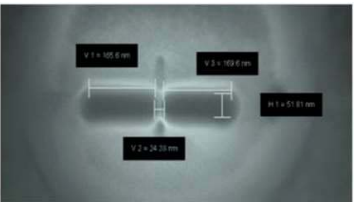


Figure 1: A gap-antenna probe fabricated by FIB-milling; the gap is 25-30 nm.

In contrast to metal nanoantennas, nanoapertures such as circular apertures surrounded by an opaque film provide truly background-free

near field sources together with a high degree of field confinement. Thus, as a second set of antenna probes we fabricated *bowtie nanoaperture antennas* (BNA) at the end facet of tapered probes. BNAs consist of two triangle openings faced tip-to-tip and separated by a small opening gap provide a superconfined spot with an intense local field and broadband response in the visible regime (Fig. 2). BNAs were fabricated at the end face of Al-coated tapered optical fibres using FIB technology. Fig. 2a-d display SEM images during the different stages of the BNA nanofabrication process. Our fabrication approach allowed for extreme reproducibility of BNA probes with the gap between the metallic arms being as small as 50 nm (Fig. 2d-f).

Although BNA probes are ideal for fluorescence correlation experiments by virtue of their large throughput, the large end-facet of the entire configuration makes it difficult for nanoimaging of fine topographic surfaces such as cells as well as accurate vertical positioning of the BNA probe with respect to the sample surface. We thus decided to extend the BNA fabrication by engineering a monopole antenna at the gap region of the bowtie (Fig. 3). The developed probe integrates three main components providing an adiabatic compression of the light down to the nanoscale: 1) tapered optical fibres tuned to diameters close to their cut-off region, 2) a bowtie nano-aperture and 3) a monopole antenna. Such a design makes optimal use of the high coupling of the optical field from

the tapered fibre into the bowtie antenna, broadband field enhancement provided by the bowtie and finally, nanofocussing and fine topographic resolution afforded by the monopole antenna.

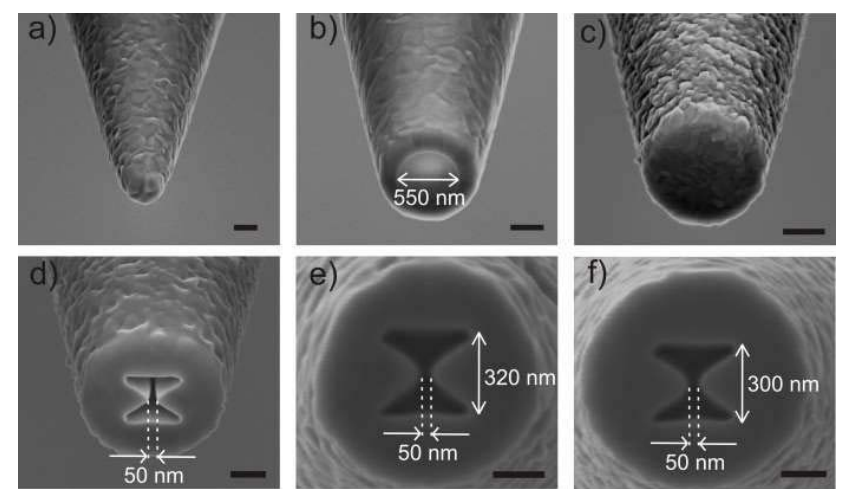


Figure 2: SEM images showing the different fabrication steps of a standing BNA probe. (a) A standard tapered fibre is coated with 5 nm of Ti and 150 nm of Al. (b) The coated fibre is milled by FIB to obtain a 500-700 nm opening diameter. (c) The end facet is coated again with a high quality Al layer of 120 nm. (d) The nanoperture is directly fabricated face-on at the end-facet of the Al layer by FIB milling. (e, f) Examples of two other BNA probes showing gap regions of 50 nm and BNA length ~ 300 nm. The scale bar is 200 nm.

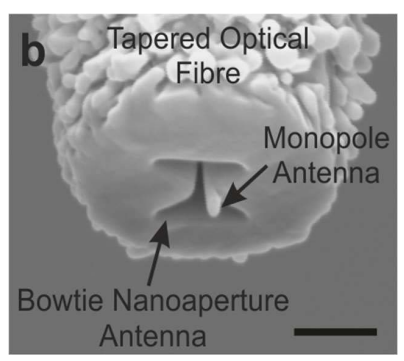


Figure 3: Representative monopole antenna engineered on BNA probes fabricated on tapered optical fibres. The tips are typically 50-70 nm in length and with tip end diameters below 30nm.

As alternative types of antennas, we also explored the potential of bottom-up *colloidally synthesized nanostars* as alternative to the top-down fabrication by e-beam and FIB. In principle, single crystalline colloidal particles have superior quality over the multi-crystalline top-down fabricated antennas. Typically the stars are 30-

60 nm with point-radius size below 10 nm, sometimes even below 3 nm. Fig. 4 shows some typical nanostars synthesized at ICFO. Interestingly, the overall size constitutes a plasmonic resonance while the spikes concentrate the field spatially. Attachment of the nanostar to the tapered fibre has been achieved by silane functionalization of the tapered optical fibre.





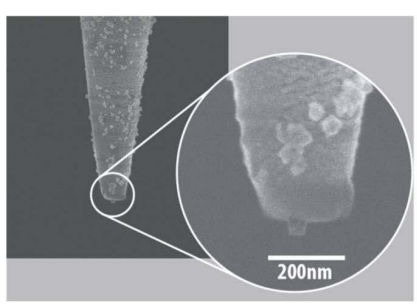


Figure 4: Left: Some typical gold nanostars, size ~ 50 nm, sub 3nm radius points. Right: a nanostar attached to a tapered optical fibre.

Finally, we also fabricated asymmetric gap antennas with resonance both for excitation and emission

and with the emission pattern depending on positioning of the emitter (Fig. 5). Such antennas can find applications in direct separation of excitation and emission in sensing or microscopy.

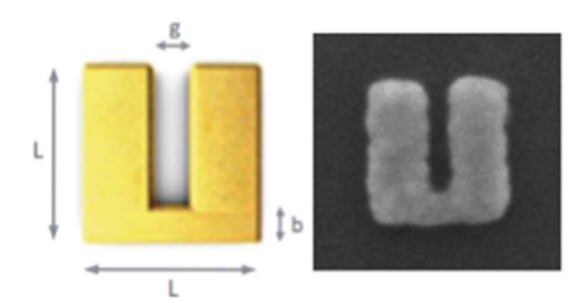


Figure 5: Asymmetric antenna: the Split Ring Resonator (SRR); scheme and e-beam fabricated gold antenna, L=250 nm, g=40 nm, b=60 nm.

Results associated to finite difference time domain (FDTD) calculations

From the starting of the project we have been performing dedicated finite difference time domain (FDTD) simulations to support and guide the most optimum antenna designs, both on probes and 2D antenna arrays. For this, we have used CST-Microwave Studio, with Lumerical and with the Boundary Element Methods. Each of these simulation tools has its specific merits and we have used them appropriately to guide the design of the different antenna geometries. In particular, we have performed FDTD simulations on the following antenna geometries: BNA on probes, monopole on BNA probes, self-standing dipole antennas on probe, monopole antennas on probes and dimer antennas embedded on nanometric boxes, both on gold and Aluminium. Moreover, we have also performed simulations to investigate how individual molecules (modelled as single dipoles) interact with the near-field emerging from these nanostructures. We have investigated effects on the control of dipole emission, directional emission, radiative and non-radiative rate enhancements, etc. More recently, we have also performed simulations aimed at investigating how antennas increase transfer rates in FRET processes using antenna configurations that include dimer-on boxes made on Aluminium and monopole-on-BNA antennas. All these simulations have been accompanied by experimental work that validate the use of these antennas, and have been published.

Results associated to experimentally measuring the optical properties of antenna probes by using them as nanoimaging tools on individual emitters.

Similarly to FDTD simulations, as new antennas were fabricated, they were first tested in terms of their optical properties before being used for biological applications. In particular, we have used fluorescent beads, quantum dots and single molecules to investigate the degree of confinement of different antenna geometries, control of the emission dipole moment of individual molecules, enhancement of the radiative and non-radiative rate of individual molecules etc. Below we show some images of the results obtained for different antenna configurations.

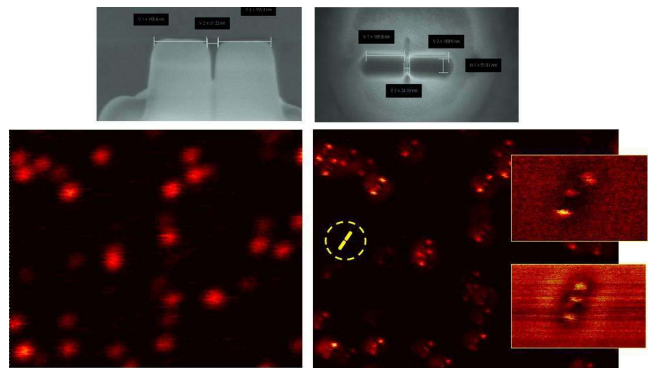


Figure 6: Assessing the degree of field confinement provided by a gap-dipole antenna using nanobeads. Top, a gap-antenna probe fabricated by FIB-milling; the gap is 25-30 nm. Bottom, confocal and gap-antenna image of the same area of fluorescent nanobeads. On the right, two magnified images of the gap-antenna response, showing 40 nm features bottom in the gap and at the extremities of the antenna.

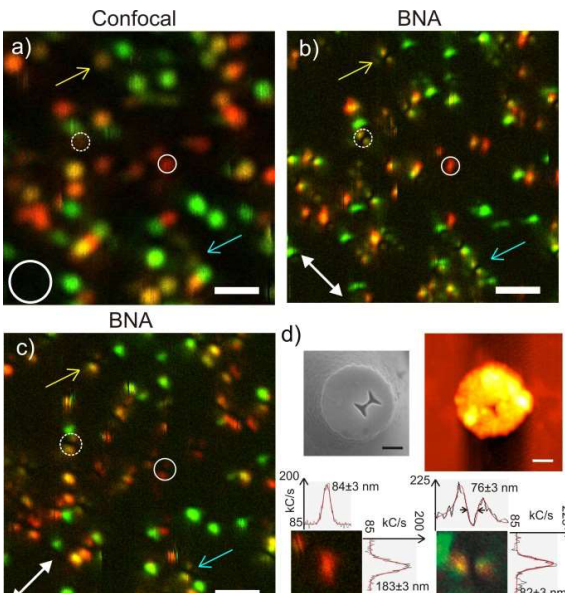
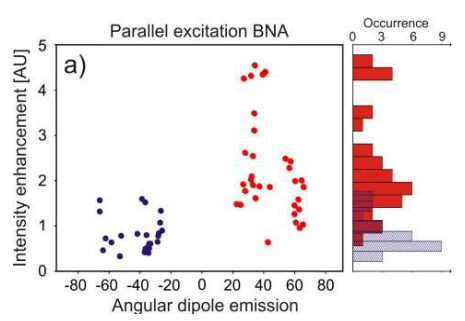


Figure 7: Assessing the 3D-near-field components of a BNA antenna using individual molecules. (a) Confocal image of individual TDI molecules embedded in a PMMA layer, excited with circularly polarized light. The image is pseudo colorcoded according to the detected signal on the APD detectors. Red corresponds to 0° (maximum collection in one APD channel), green to 90° (maximum collection in the orthogonal APD channel) (b,c) Counterpart images of the same sample area obtained with the BNA probe excited parallel (b) and perpendicular (c) to its metallic arms. The scale bars are 1 um. (d) The upper panels show a SEM image of the BNA (left) and a topographic feature obtained simultaneously with scan showing the end-facet of the BNA (right). The scale bars are 200 nm. The lower panels show cross-sections of two representative single molecules, oriented parallel to the BNA metallic arms (left) an out-of-plane orientation (right).



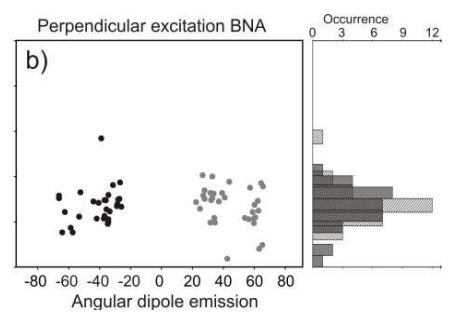


Figure 8: Assessing the degree of BNA enhancement using single molecules. Intensity enhancement I_e vs. in-plane angular emission of individual molecules, for excitation of the BNA parallel (a) and perpendicular (b) to its metallic arms. Each individual dot corresponds to a single molecule. Data have

been compiled on multiple sets of images, each set containing confocal and BNA images for different BNA excitation polarization conditions of the same scanning area.

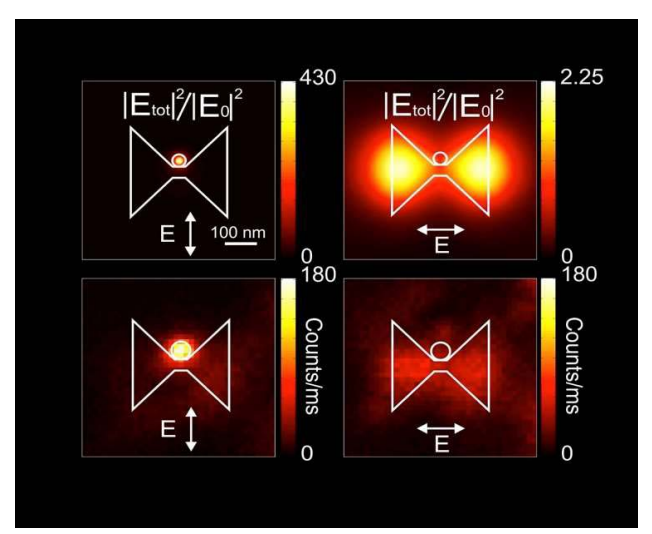


Figure 9: Assessing the degree of nanofocussing & field enhancement of a hybrid nanoantenna (monopole on BNA probe) using individual nanobeads. Upper raw: Normalized intensity (E_{tol}^2/E_0^2) calculated by FDTD in a xy-plane at 10 nm away from the monopole tip, for transversal (Left) and longitudinal (right) excitation polarization (λ =633nm) of the BNA. The BNA gap is 30nm, the monopole length is 70nm with tip diameter of 30nm. Lower raw: Experimental near-field images of a 20nm fluorescence bead scanned under the hybrid nanoantenna upon transversal (left) and longitudinal (right) excitation polarization.

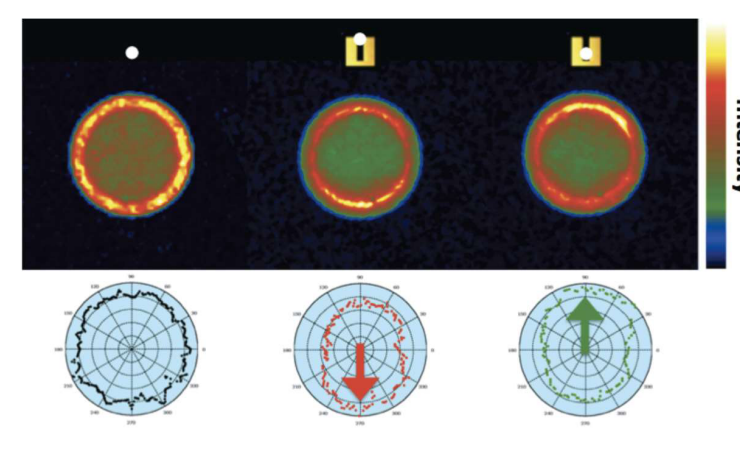


Figure 10: Assessing the performance of a scanning split ring resonator (SRR) antenna by measuring the angular emission patterns of a nanobead. This is a "simple" single element antenna, which still sustains several modes. The symmetric angular pattern of the bead shifts forward or backward depending on position in the gap of the asymmetric antenna.

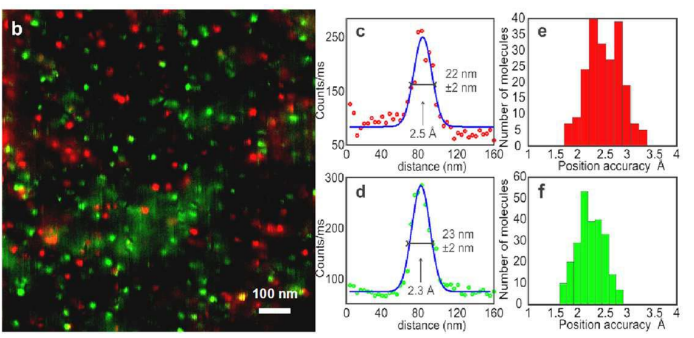


Figure 11: Assessing the degree of confinement and localisation precision provided by a monopole-on-BNA antenna. (b) Dual colour nanoimage of DiD (green) and DiI (red) molecules embedded in a thin polymer layer. (c,d) Line profiles over two different molecules, DiI (c) and DiD (d) yielding tru optical resolutions of ~20nm for both wavelengths. (e,f) Localization accuracies obtained over hundreds of DiI (e) and DiD (f) molecules. The coordinate of each fluorescent spot is calculated with 2Å precision and colour-coded plotted according to the emission wavelength.

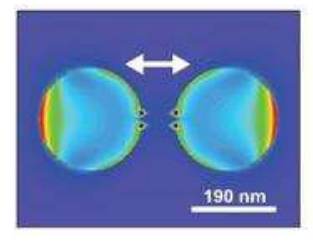
Workpackage 2: Development of novel 2D photonic antenna arrays for biophotonics applications and biosensing.

As stated in the original proposal, this WP addresses the development of 2D photonic antenna arrays with improved performance for biophotonics applications and biosensing. To this end, we have focused on two main objectives: 1) to tune the geometry and shape of 2D antenna arrays for efficient light capture and nanofocussing, directional control and antenna-mediated spectral selection; 2) to develop new methods to enhance single molecule fluorescence analysis and fluorescence correlation spectroscopy (FCS) on 2D antenna arrays different strategies, including physical masks to reduce background, chemical quenching to tune the emitter's quantum yield, polarization modulation to extract the relevant signal from the antenna gap region and non-linear wave mixing illumination to improve the non-linear contrast on the gap region.

Results associated to different 2D antenna designs for efficient light capture, nanofocussing and field enhancement.

Among different plasmonic antenna designs, the *double nanohole* (DNH) structure (Fig. 12) is attracting much interest thanks to its distinctive advantages of narrow gaps, high enhancement and efficient background screening. While DNH structures have been broadly applied for optical trapping of nano-objects, there has been no report of their use to enhance the fluorescence of single molecules. We have demonstrated the effectiveness of double nanohole structures to enhance single molecule fluorescence detection at high concentrations. Using FCS, we measured the near-field apex volume to \$\sigma^3/3800\$, realizing a volume reduction of 7000-fold as compared to diffraction-limited confocal setups. The high intensity confinement goes with fluorescence enhancement up to 100-fold, together with microsecond transit time, 30-fold LDOS enhancement and single molecule sensitivity at concentrations exceeding 20 micromolar. This work provides a complete quantitative characterization of the near-field detection volumes and the fluorescence enhancement in a DNH antenna. We relate our experimental data to numerical simulations and thoroughly describe the fluorescence photokinetic rates in the DNH. Additionally, the DNH provides an efficient design to reach nanometer confinement of light, with a comparatively simple nanofabrication.





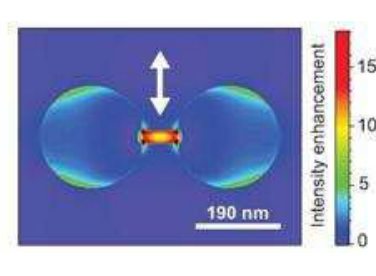
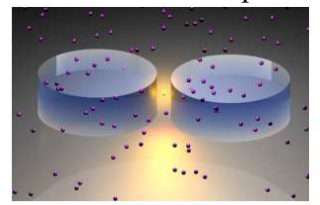
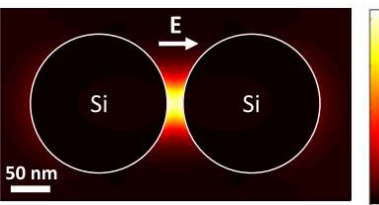


Figure 12: double nanohole antenna for near-field fluorescence enhancement

Fluorescence single molecule sensors based on plasmonic metal nanostructures are currently limited by the non-radiative energy transfer between emitters and free electron gas and by the Joule heating caused by the excitation laser beam. A new paradigm is needed to design optical antennas without these limitations so as to implement reliable and cost effective molecular sensors with on-chip and CMOS compatible nanophotonic devices. Silicon-based nanophotonics is currently one of the very active approaches to meet this goal. Within NANO-VISTA we reported the first *all-dielectric nanoantennas* (Fig. 13) able to enhance the fluorescence signal of individual molecules at biological concentrations. We designed and fabricated all-silicon nanogap antennas that confine light by 3600-fold below the diffraction limited confocal volume and provide fluorescence enhancement up to 270×. This gives the first experimental evidence that silicon nanoantennas can achieve fluorescence enhancements above 200-fold and allow the detection of individual molecules at micromolar concentration using dielectric materials only. We have demonstrated that the fluorescence enhancement results from a combination of excitation intensity and radiative rate enhancement within the nanogap region. By combining a large set of experimental techniques with thorough

numerical simulations and by measuring for two different molecules, we have quantified the different contributions to the fluorescence enhancement in this new antenna material. These results open new routes to implement high sensitivity molecular (bio)sensors with on-chip photonic devices that are CMOS compatible.





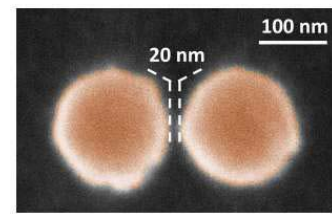


Figure 13: all-dielectric silicon nanoantenna

Within NANO-VISTA we also explored other 2D designs such as *finite-sized hexagonal arrays of nanoapertures* milled in a gold film. We have demonstrated that already small lattices enable highly directional and enhanced emission from single fluorescent molecules in the central aperture, while the directionality is set by the plasmonic crystal band structure. This realization of plasmonic phase array antennas driven by single quantum emitters opens a flexible toolbox to engineer fluorescence and its detection. In terms of directionality control and in addition to the hexagonal arrays, we also demonstrated the successful fabrication of *Yagi-Uda antennas* and *splitting ring resonators*, which both show a highly directional emission pattern, and in the case of the splitting ring resonator, maximum forward emission and broadband response, i.e., superior to the Yagi-Uda performance.

All the 2D antenna array designs mentioned above have been successfully tested on individual molecules in terms of localization, field enhancement and directional control showing their absolute superiority as compared to standard optical techniques. Moreover, these devices are particularly suitable to enhance the emission of weakly fluorescent molecules. This is for instance the case of biological light-harvesting systems (LH2), which capture effectively the incident sunlight, yet they are optimized for energy transfer, where any light emission constitutes a loss channel. By coupling single LH2 complexes resonantly to gold nanoantenna arrays we demonstrated that the quantum efficiency could be enhanced from only a few percent to 50% with 20ps decay time. As result, almost 1000 times more emission was collected from a single complex (Fig. 14).

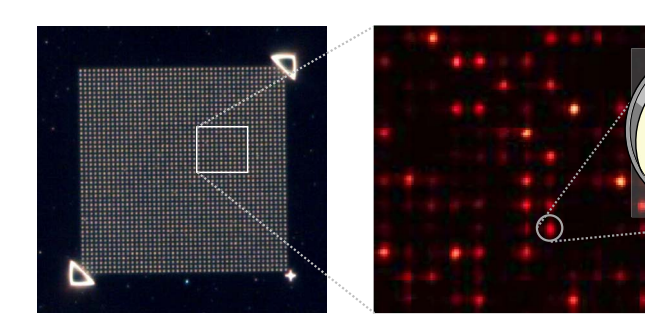


Figure 14: Enhancement of single light harvesting complexes on resonant antenna array. Left; optical image of array of 2500 gold antennas, each 160 nm length x 50nm width (□/2 antenna for □=800-850 nm). Middle confocal fluorescence image, showing bright individual light-harvesting complexes on the antenna array; right sketch of the complex at an antenna hotspot.

Results regarding new methods to enhance single molecule fluorescence analysis and FCS on novel 2D antenna array designs.

We have explored and demonstrated several useful strategies to enhance single molecule analysis and FCS detection on 2D antenna arrays. One of the most useful strategies has been the combination of external chemical fluorescence quenchers (such as methyl viologen) to tune the emitter's quantum yield together with physical masks to reduce background contribution from fluorescent molecules outside the antenna gap region. In practice, the most efficient design consisted on a gap-antenna inside a nano-aperture (antenna-in-box) (Fig 15). The different components of the "antenna-in-box" have complementary roles: a central gap-antenna creates the hot spot for enhancement, while a surrounding nanoaperture screens the background by preventing direct excitation of molecules

diffusing away from the central gap region. In addition, the use of the quencher reduces the quantum yield of Alexa 647 from 30% down to only 8%, contributing to the suppression of additional background from diffusing molecules within the nanobox.

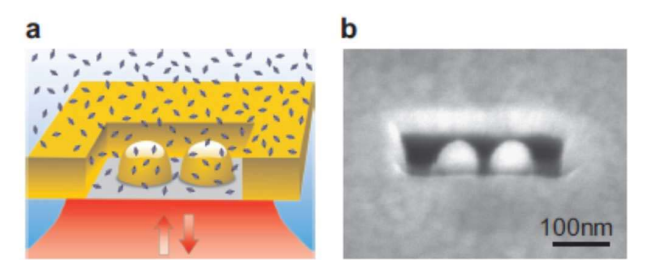
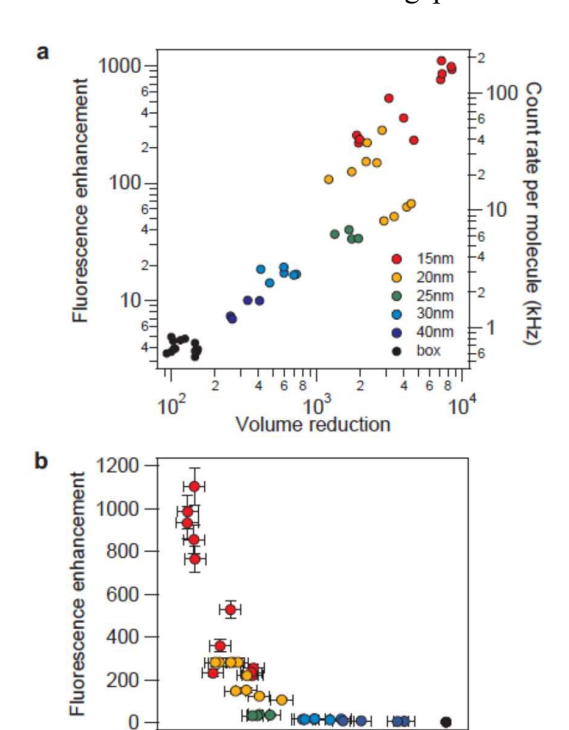


Figure 15: (a) Schematic of dimer gap antenna inside a rectangular aperture. The device is milled in a gold film on a glass substrate, and covered by a solution containing fluorescent molecules at micromolar concentration. (b) Scanning electron microscopy (SEM) image of a fabricated nanoantenna.

By means of FCS we demonstrated unprecedented fluorescence enhancement and volume reduction. Local field enhancement was found to critically depend on the antenna gap size. As example, Fig. 16 shows scatter plots of the fluorescence enhancement as a function of the volume reduction and gap size for 59 nanoantennas with gap sizes ranging from 12 to 40 nm. Clear correlation between



10

20

30

Gap size (nm)

40

fluorescence enhancement and volume reduction consistent with field localization in the gap region is observed. The nanoantennas with smallest gap sizes yield the highest fluorescence enhancement and volume reduction, up to 1100x enhancement factor and 8550x volume reduction compared to confocal excitation. The best confinement achieved amounts to a volume down to 58 zL for a gap size of 12 nm. Remarkably, this detection volume is four orders of magnitude smaller than the diffraction limit. These results demonstrate the capability and superiority of nano-antenna devices for efficient sensing platforms single molecule analysis at micromolar concentrations.

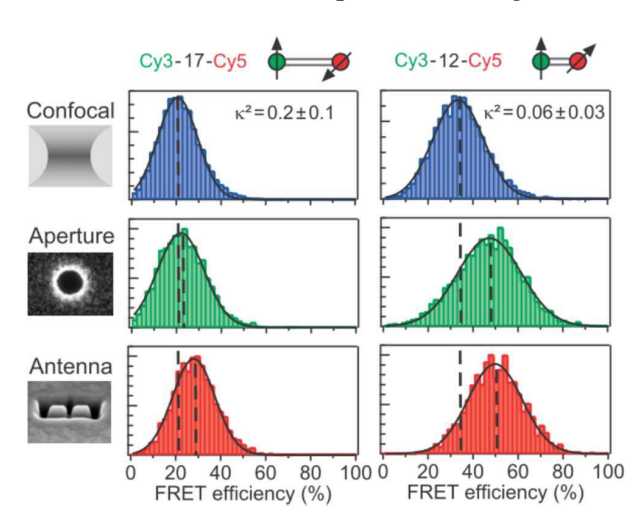
Figure 16: (a) Scatter plot of fluorescence enhancement versus volume reduction as compared to the diffraction-limited confocal set-up. The different markers represent different antennas tested, while the colour indicates the nominal gap size used for the fabrication. (b) Scatter plot of the fluorescence enhancement factor as a function of gap size calibrated by FCS.

Confining light at a spatial scale comparable to the molecular size also opens new opportunities to enhance Förster resonance energy transfer (FRET), which is a ubiquitous phenomenon governing the energy exchange at the nanoscale and is widely applied in biochemistry, organic photovoltaics, and lighting sources. We fabricated our antenna-on-box design on Al such that we could enhance single molecule FRET. Our single-molecule experiments reported a 10-fold increase in the photonic density of states together with an unprecedented 5-fold enhancement of the FRET rate. Importantly for practical applications, our work demonstrated that optical antennas could extend the spatial range of FRET to distances where dipole-dipole interactions would otherwise be too weak to produce detectable FRET signals. As such, we introduced clear design rules to enhance the FRET rate with a nanoantenna. This understanding is essential for the future development of nanophotonics to control

Box

energy transfer on nanometre distances for applications in photovoltaics, organic lighting sources and importantly, in biosensing.

We also extended our FRET experiments to enable forbidden energy transfer by means of nanoantennas. In particular, we have shown a novel use of plasmonic nanoantennas to exploit the orientation dependence in FRET in our advantage. We demonstrated that the nanoantenna creates favourable conditions for the donor dipole radiation, generating strongly inhomogeneous and localized fields in the nanogap which open new energy transfer routes, overcome the limitations from the mutual dipole orientation, and ultimately enhance the FRET efficiency. While several previous works on FRET with nanophotonic structures addressed the link between FRET and the local density of optical states (LDOS), our work has been the first to bridge the gap between FRET orientation effects and near-field optics, showing that FRET is allowed in the nanoantenna even for



perpendicularly oriented donor and acceptor pairs (Fig. 17). Our findings provide a new strategy to use nanophotonics to reveal FRET interactions that would otherwise be impossible to probe using diffraction-limited microscopes. This non-explored aspect of nanoantennas has wide applications from fundamental near-field optics to bio-applications of single-molecule FRET.

Figure 17: Improvement of FRET efficiency up to 50% for Cy3-Cy5 FRET constructs in nanoantennas.

One of the key factors that control the nanoscale optical properties of photonic antennas is the polarization of incident electromagnetic fields, which influences the amplitude and polarization of scattered fields. By varying the excitation polarization, one can not only tune the spectral properties of metal nanostructures of complex shapes, but also the spatial and vectorial properties of their local fields at the nanoscale. Along these lines, we have developed a method of polarized nanoscopy that exploits sub-diffraction resolution information down to a few tens of nanometres. Even though the resulting image is diffraction-limited, the information gained by polarization-induced modulation provides a higher level of selectivity that is directly related to vectorial optical responses at a scale below the diffraction limit. We show that polarized nonlinear nanoscopy permits to spatially map the vectorial nature of plasmonic nonlinear optical interactions in nanostructures (Fig. 18).

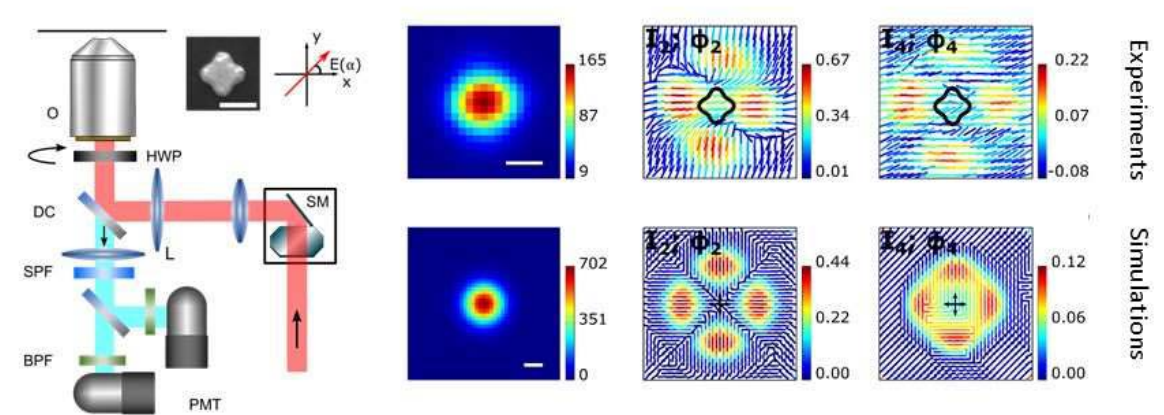


Figure 18: Polarization resolved nonlinear nanoscopy

Workpackage 3: Large scale, high throughput nanofabrication of antenna arrays for life science applications.

As stated in the original proposal, this WP concentrates on designing routes for large-scale, high throughput nanofabrication of antenna arrays compatible with life science applications. To that end, we have focussed on two main objectives: 1) the implementation of micro- and nanofabrication techniques for high throughput fabrication of 2D arrays at large physical scales (millimetres) with optimum geometries; and 2) to provide routine fabrication routes of the antenna arrays having the following performance: optical properties consistent with those of antennas, design flexibility and compatibility with biomolecules, rapid and cost efficient fabrication. Below we present the major breakthroughs obtained in this WP.

According to the original workplan and associated deliverables, metal deposition through nanostencils was envisioned as an ideal candidate for the fabrication of large-scale plasmonic antennas at low cost, therefore well suited as a basis for the development of a biophotonic platform. One promising antenna design (developed in WP1) consisted on aperture-type metal structures rather than isolated particle-type nanoantennas. We thus implemented a stencil lithography approach based on metal etching rather than deposition. The optimization of the process enabled blurring-free patterning of BNA antennas over millimetric surfaces without the requirement for gap reducing schemes such as compliant stencils (Fig. 19). We tested the usefulness of these antennas by recording the diffusion of individual lipids on living cell membranes (more details in WP5)

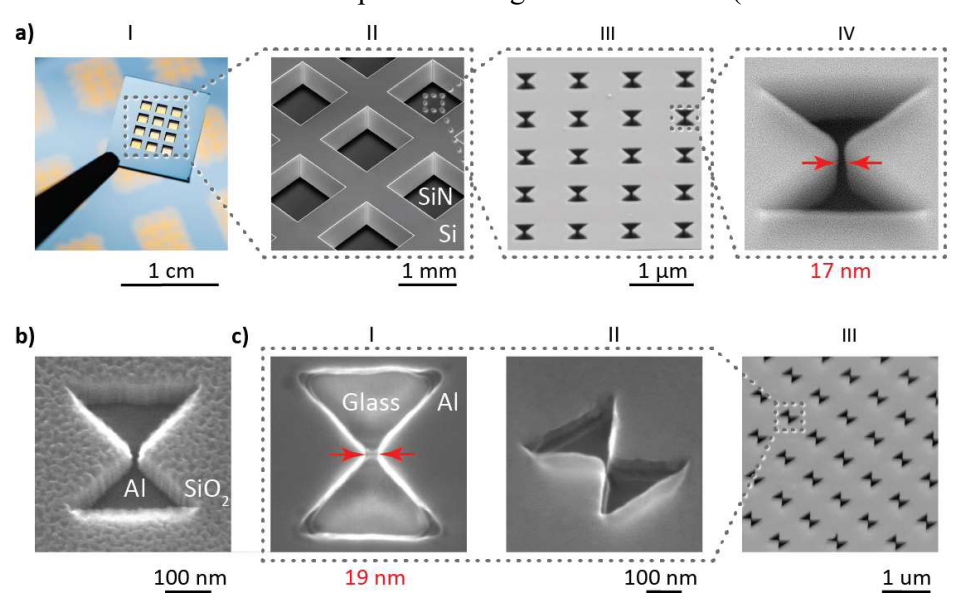


Figure 19: a) Photograph of a nanostencil: the silicon frame supports 12 patterned silicon nitride membranes and details of the membrane area and backside machining of the silicon, together with SEM images of a dense antenna array on the silicon nitride membrane, b and c) high resolution images of single apertures in the stencil including final protection by atomic layer deposition of alumina. The gap width is 17 nm. The scale bars are, respectively, 1 cm, 1 mm, 1 µm, 100 nm. SEM images all at 45° tilt.

In addition to BNA geometries, we have focused on other designs. Following large scale requirements, repeatable antenna performance and ultimate near field enhancement, we investigated a novel lift-off procedure based negative electron beam resists enabling throughputs order of magnitude higher than typically achieved via FIB along with higher resolution (Fig. 20). The control of electron beam lithography and gold evaporation at low temperatures allowed the fabrication of dimer-in-box antennas with gaps with high repeatability. Upon lift-off of the metal layer, the antennas were stripped from the substrate with a UV curable polymer in order to obtain a flat surface and position the narrow gap region at the surface. These antennas were additionally fabricated on electron transparent silicon nitride membranes for high-resolution metrology by transmission electron microscopy. The dimer gap width, that localizes a bright hot spot for fluorescence enhancement, could be successfully tuned from ~50 nm down to 10 nm, which is impressive. TEM statistics show the low line edge roughness of the structures along with minimal gap size dispersion. Full optical characterization has been performed with FRESNEL & ICFO-SMB partners and the

major results are reported in WP5. With additional patterning of the substrate prior to metal deposition and further processing we also showed the possibility to include three dimensional elements protruding out of plane in order to extract the antenna near field at an accessible position for the target fluorescent sample (Fig. 21).

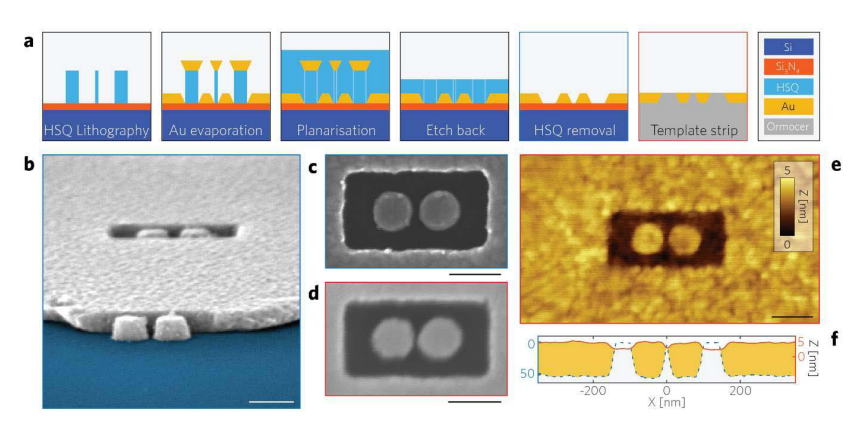


Figure 20: a) Different fabrication steps of flat 2D antenna arrays. b) Tilted SEM view of an opened antenna-in-a-box before template stripping. c) A similar structure is imaged from the top before and after d) template striping. The antenna surrounding is filled by the UV curable polymer as seen in the AFM image e) showing less than 5 nm residual topography. f) AFM profiles before (dashed blue) and after (red) template stripping of the 50 nm-thick gold structure. Scale bars are 100 nm.

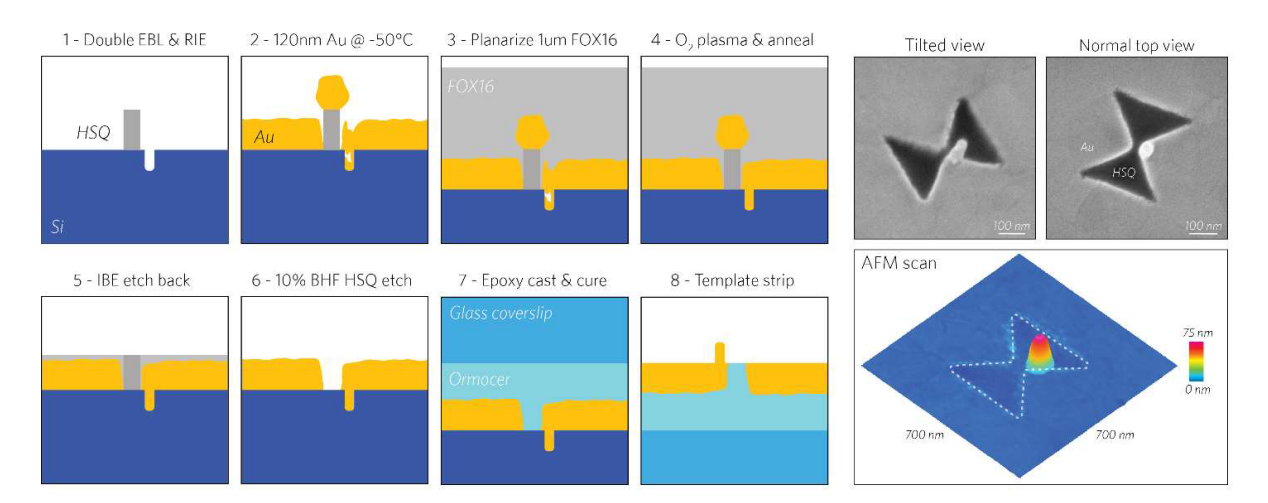


Figure 21: Schematic representation of the modified process enabling additional 3D features in the antenna geometry and corresponding SEM (upper images) and AFM (bottom) images of the fabricated antennas.

Although aperture antennas offer high signal-to-background ratios, "positive" type geometries are also of interest due to their strong field enhancement. Standard fabrication methods are usually based on EBL and lift-off that have resolutions in the order of 10nm. Such processes also require adhesion layers that have been shown to damp the plasmon resonance. Moreover, the polycrystalline nature of the deposited metal thin films is also seen as a source of losses and resonance broadening. To overcome these limitations, we have developed and investigated the assembly of chemically synthesized single crystal gold nanoparticles. This technique based on the generation of nanoparticle accumulation at the three phase contact line of a colloidal drop, also called coffee-ring, via solvent evaporation. Upon formation of the accumulation region, the drop is dragged over a patterned template and the particles assemble in the grooves as shown in Fig. 22a. Control over the contact angle through surface silanization and surfactant choice allows selective assembly at high yields over 90% over large areas with inter-particle distances below 2 nm. While spherical nanoparticles with complete symmetry are most conveniently assembled, elongated rod-type colloids are also positioned with additional the control over the particle orientation.

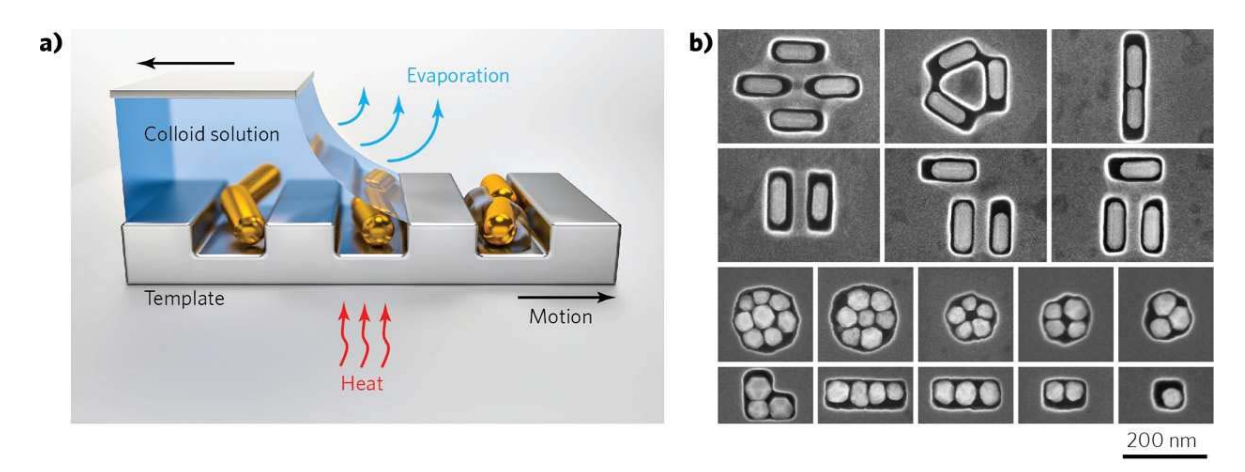


Figure 22: a) schematic view of the nanoparticle assembly process. Evaporation drives the particles to the contact line and motion of the drop relative to the template enables assembly over sequential template grooves. b) collection of nanoparticle ensembles assembled via capillarity assisted nanoparticle assembly.

Beyond proof-of concept fabrication of a broad range of antenna geometries as shown in Fig. 22b, the capillarity assisted nanoparticle assembly (CAPA) process was thoroughly characterised. The influence of the process parameters along with precise control of the trap geometry in all three dimensions allowed us to design rules to establish different geometries. We first investigated the influence of the trap cross-section beyond a simple rectangular profile with vertical sidewalls. Among others, the fabrication of funnelled traps allowed us to assemble 120x40 nm gold nanorods with high yield in all orientations, with a standard deviation from the desired angle of less than 2°. The fabrication of traps with controlled profiles along with nanoparticle assembly has been carried out on SiO₂ and glass substrates for full compatibility for biology & fluorescence requirements. We have fabricated and defined optimal geometries in collaboration with CNRS partners for fluorescence enhancement measurements on nanorod dimer structures with gaps below 10nm. Fabrication and assembly of nanoparticles on suspended membranes has also been carried out for TEM metrology and electron energy loss spectroscopy measurements.

The use of 2D plasmonic antenna arrays for living cell bio-imaging applications requires the manipulation of living cells on the plasmonic antenna chip. Specifically, the two crucial requirements are cell positioning on the antenna arrays, and maintaining the cell viability to ensure cell adhesion on the antennas that naturally advances the cell membrane, and therefore the target bio-molecules, to the vicinity of the antennas. To meet these requirements we proposed to use an integrated microfluidic system that can be aligned and bonded on the antenna array chip.

The main idea is to have a hydrodynamic cell trapping method that takes place on the structured parallel microfluidic channels. A 3D rendered model of the proposed cell-arraying platform, where the cells are sequentially trapped in the parallel microchannels, is shown in Fig. 23a. The inlet and outlet are designed to provide enough media to the cells during long-term static cell culturing. The distribution of cell trapping/accommodating chambers in the microfluidic channels is assigned to align with the antenna arrays. Using this approach we have succeeded in arraying 400cells/device. The dark-field microscope image of the MIA PaCa-2 cells arrayed at the trap positions is shown in Fig. 23b. We achieved 70% trapping efficiency in short cell loading times (1-4 min), with minimal mechanical stress on the cells during and after the cell insertion. Moreover, the arrayed cells are observed under microscope with stage-top incubators to prove the compatibility of the method for day-scale on-chip static cell culture. We did not observe any viability issue during the day-scale (2 days) static cell culture periods. Moreover, we measured the time dependent proliferation rate of the MIA PaCa-2 cells and their doubling times were compatible with the literature, indicating that the

arrayed cells continued their natural growth cycle and our microfluidic cell manipulation method does not impose any intervention to the on-chip cell culture.

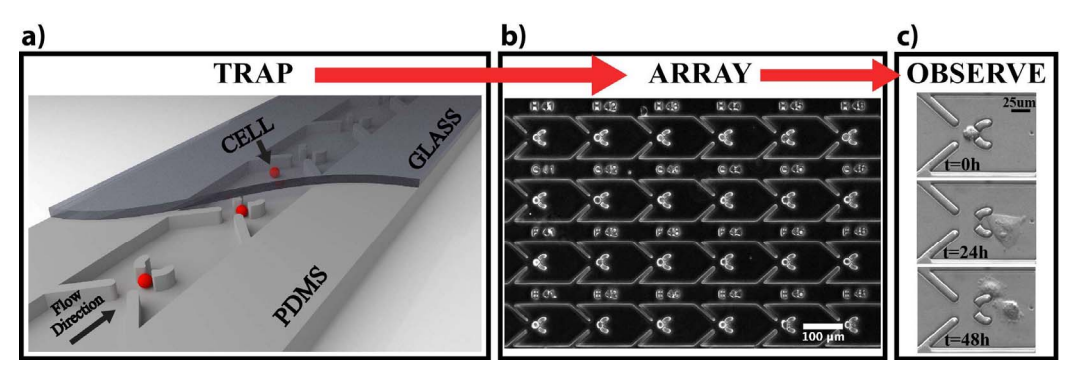


Figure 23: Microfluidic on-chip cell manipulation a) 3D rendered model of the hydrodynamic single-cell isolating structured microfluidic channel where the cells are sequentially trapped b) Dark-field microscope image of the MIA PaCa-2 cells showing a portion of the cell array c) Time lapse, phase contrast microscope images of arrayed single MIA PaCa-2 cell cultured in the microfluidic device.

We then assembled the cell trapping microfluidic platform to two types of plasmonic chips with arrayed sensing zones: 1) Self assembled Au nanoparticles (NP) on Si (Fig. 24a) 2) Stencil patterned Al BNA array on glass (Fig. 24b). The PDMS microfluidic cell trap chambers are aligned to the prepatterned nanostructures under microscope and irreversibly bonded on the chips. As seen in Fig. 24, micron-scale accuracy is achieved in this chip alignment process. Next, living cell suspension is inserted into the inlet and cells are positioned on the dedicated Au NP sensing zones. Fig. 24a shows the cell trap chambers assembled on Au NP arrays and the aligned living cell arrays on them.

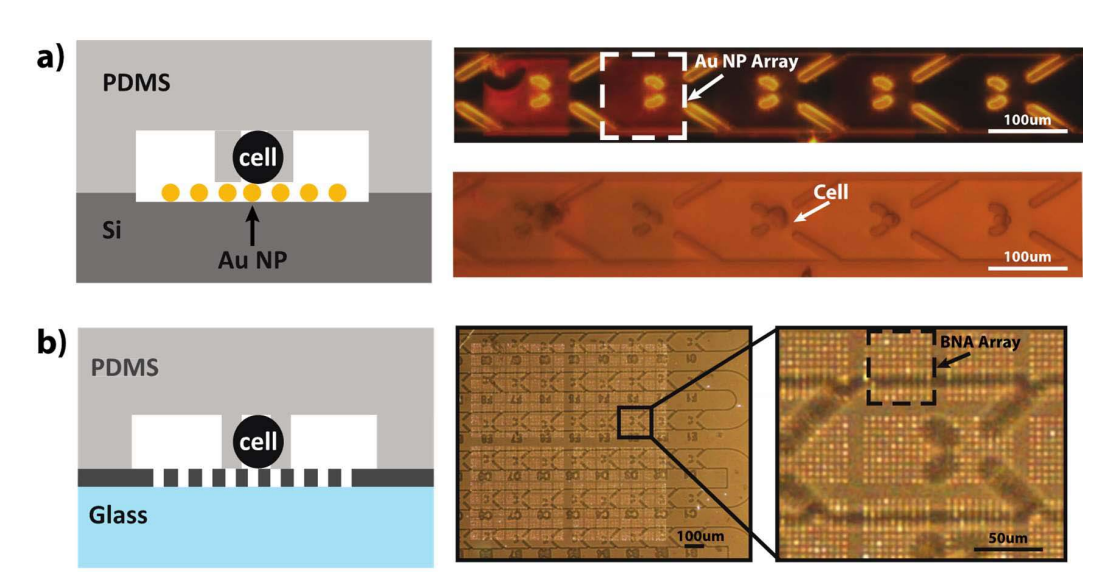


Figure 24: Living cell arrays on the plasmonic chips. PDMS microfluidic cell trapping platform is aligned and bonded on a) self-assembled Au NP array zones on Si-substrate b) stencil patterned Al BNA array zones. Bright-field image.

Workpackage 5: Implementation of antenna geometries for nanoimaging and nanospectroscopy in in-vitro and in live cell research.

According to the original proposal, this WP is targeted to the implementation of different antenna geometries as bionanophotonic tools for nanoimaging and nanospectroscopy in living cells. To this end, WP5 has focused on two specific objectives; 1) the application of antenna probes for single molecule detection and super-resolution multi-colour imaging on intact cell membranes using a

scanning system platform; and 2) the application of antenna probes and 2D antenna arrays for nanofocussing FCS and FCCS on living cells.

Results regarding the application of antenna probes for single molecule detection and superresolution multi-colour imaging on intact cell membranes.

For super-resolution imaging we have mainly concentrated on monopole-on-BNA probes (so called hybrid antennas) as they provide broadband response and high degree of field confinement. As already mentioned in WP1, we showed that with our improved hybrid design the optical resolution in two colours is around 20nm (Fig. 11). Aside from the increased resolution, these types of antennas are sharper and have a narrow end-face, facilitating studies on cell membranes. Moreover, we successfully demonstrated various antennas on probe configurations for super-resolution nanoimaging of individual molecules of two different colours, by exciting simultaneously the hybrid antenna with 488nm and 647nm, obtaining true optical resolution of 20nm in both wavelengths together with sub-nanometre localization accuracy (0.2nm) (see Fig. 11).

One of the major requirements to fully exploit the broadband properties of BNA and hybrid antennas is the implementation of multicolour excitation and detection scheme fully compatible with the imaging platform. We thus implemented a novel approach that relies exclusively on the excitation properties of the fluorophores instead of their fluorescence emissions. In our technique the intensities of all of the excitation lasers are independently modulated at their own unique frequencies (Fig. 25a), launched into our combined confocal/NSOM platform and focused to a diffraction-limited spot using a high-NA objective, or guided to the back-end of the optical fibre containing the hybrid antennas. The fluorescence is collected by the high-NA objective, directed through a set of notch filters chosen specifically to reject the excitation wavelengths used in the experiment and sent to the detector. A fast Fourier transform (FFT) converts the digital time-domain signal from the APD into an analogue frequency domain signal, from which the amplitude at each modulation frequency is extracted (Fig. 25b). The frequency-domain amplitudes are plotted in real time to generate excitation maps for each wavelength as the sample is laterally raster-scanned across the excitation spot (Fig. 25c). For unequivocal determination of the spectra and spatial distributions of the fluorescent species in the image we also developed a user-friendly spectral unmixing algorithm that utilizes a non-negative matrix factorization (NMF) and can operate on *underdetermined* data sets.

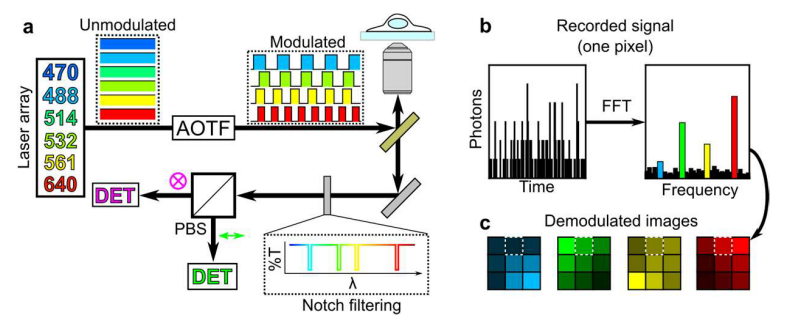


Figure 25: Experimental setup for excitation-multiplex multicolour microscopy.

(a) Block diagram of the main optical components of the setup. For simplicity we only show the confocal excitation path. (b) The fluorescence detected by each APD is converted into a digital data stream. A FTT is performed on a pixel-by-pixel basis to convert the photon signal into the frequency domain, where the amplitudes of the signal at each modulation frequency are measured

and plotted (c) as pixel intensities in individual images for each excitation source.

We validated our multicolour approach on a variety of different samples & conditions, including fixed cells labelled with up to 6 different colours and on multicolour single molecule detection both in confocal and antenna-excitation conditions. A representative four-colour image of HeLa cells in shown in Fig. 26. The spectrally unmixed data yield clear distribution maps of each organelle with intensities that are proportional to the concentration of the fluorophore at each pixel.

We then moved to dual-colour nanoscale imaging of fixed intact cells using our hybrid antennas together with our excitation-multiplexing approach. As proof-of concept studies we focussed on GPI-APs and pathogen receptors (DC-SIGN) expressed on immature dendritic cells (imDC).

Simultaneous dual colour confocal and nanoscale imaging of GPI-AP (blue) and DC-SIGN (red) on imDCs obtained with the antennas are shown in Fig. 27.

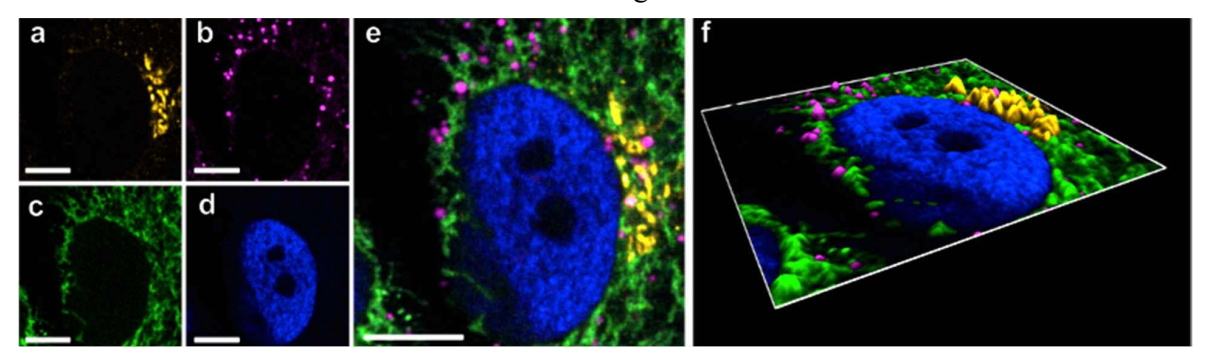
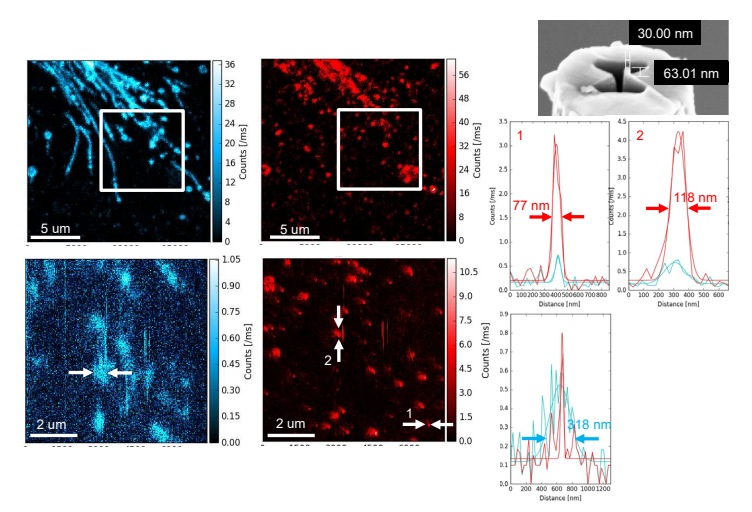


Figure 26: Representative simultaneous multicolour excitation-multiplexed microscopy of four different cellular structures in HeLa cells using four excitation lasers at 470, 514, 561, and 640 nm. (a-f) Spectrally unmixed data showing the distributions of the Golgi complex (a, yellow), lipid droplets (b, magenta), mitochondria (c, green), and nucleus (d, blue), with composite (e) and volumetric (f) images. Scale bars, $10 \square m$.

Fluorescence line profiles of the DC-SIGN channel show the superb improvement in optical resolution & intensity signal as obtained by antennas. The sizes of the fluorescence spots vary from 70 to 150nm consistent with the reported DC-SIGN nanocluster sizes. To our knowledge, these are the first results that demonstrate the capability of photonic antennas for nanoscale imaging of



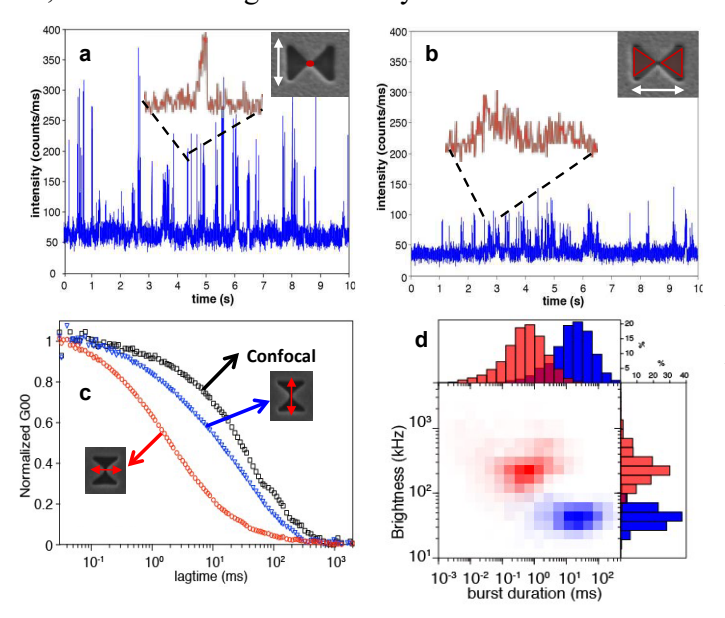
receptors on the cell membrane. Nevertheless, the signal arising from the GPI-APs is quite weak, and the spot diameters are significantly larger than the ones expected with these sharp antennas. We are currently investigating these unexpected results.

Figure 27: Representative dual-colour confocal images (upper row) of GPI-APs (blue) and DC-SIGN (Red) on imDCs. Bottom row: Dual colour hybrid-antenna imaging of GPI-APs and DC-SIGN obtained upon zooming on the box regions marked on the confocal images. Right: SEM image of the antenna probe used in these experiments and representative line profiles of DC-SIGN (red traces) and GPI-APs (blue line).

Results regarding the application of antenna probes and 2D antenna arrays for nanofocussing FCS and FCCS in in vitro conditions and on living cells.

In the case of antenna-on-probes, we demonstrated the feasibility of BNA antenna probes to record the lateral mobility of PE lipids labelled with atto647N on the membrane of living CHO cells. Fig. 28a shows a representative fluorescence trajectory over time obtained with a BNA probe excited with transversal polarization (see inset). The different fluorescent bursts correspond to the passage of diffusing lipids under the illumination of the BNA. Fig. 28b shows a representative trajectory on the same sample position but for longitudinal polarization excitation of the BNA. Remarkably, the bursts are shorter and of higher intensity for transversal excitation consistent with the local confinement and field enhancement provided by the BNA under these excitation conditions. Multiple time traces were autocorrelated to generate FCS curves under confocal and BNA excitation, both for longitudinal and transversal polarization (Fig. 28c). Analysis of the FCS curves revealed that for longitudinal BNA excitation, the number of PE molecules is 13 ± 5 and transient times are $\Box_D = 11.9\pm 3.2$ ms. For transversal polarization excitation, N= 6 ± 5 and $\Box_D = 1.8\pm 0.5$ ms. These results demonstrate the

excellent lateral confinement of the BNA upon transversal excitation. Based on these values we estimate that the excitation area of the BNA corresponds to approximately 48nm for transversal polarization, which is at least one order of magnitude higher confinement compared to confocal. Given the low backgrounds afforded by BNA antennas we could also discriminate individual fluorescent bursts and analyse their intensity and burst width (Fig. 28d). Consistent with the FCS data, shorter and higher intensity bursts are obtained when the BNA is excited under transversal



polarization, compared to longitudinal polarization consistent with the high confinement and field enhancement of RNAs

Figure 28: FCS of PE lipids on living CHO cells using BNA antenna probes. (a) Fluorescent time trace (1ms bin) of PE-atto647N obtained with a BNA probe (see inset) under transversal polarization excitation. (b) Equivalent time trace obtained with the BNA excited with longitudinal polarization. (c) FCS curves obtained after averaging 5 different fluorescence trajectories in each case, for confocal (black), longitudinal (blue) and transversal polarization (red) of the BNA. Notice that the curves are shifted towards shorter times as the illumination volume is reduced. (d) Two dimensional plot of the burst duration vs. burst brightness for BNA excitation under longitudinal (blue) and transversal (red) polarization.

We also demonstrated FCCS at the nanoscale using BNA antenna probes. In this particular case, we focused on the mobility of a pathogen recognition receptor (DC-SIGN) to resolve molecular interactions between individual DC-SIGN molecules. The results shown in Fig. 29 demonstrate the feasibility of measuring co-diffusion of individual molecules at the nanometre scale by means of antennas, making these bright nanostructures promising candidates for a quantitative study of the endogenously concentrated cellular membrane.

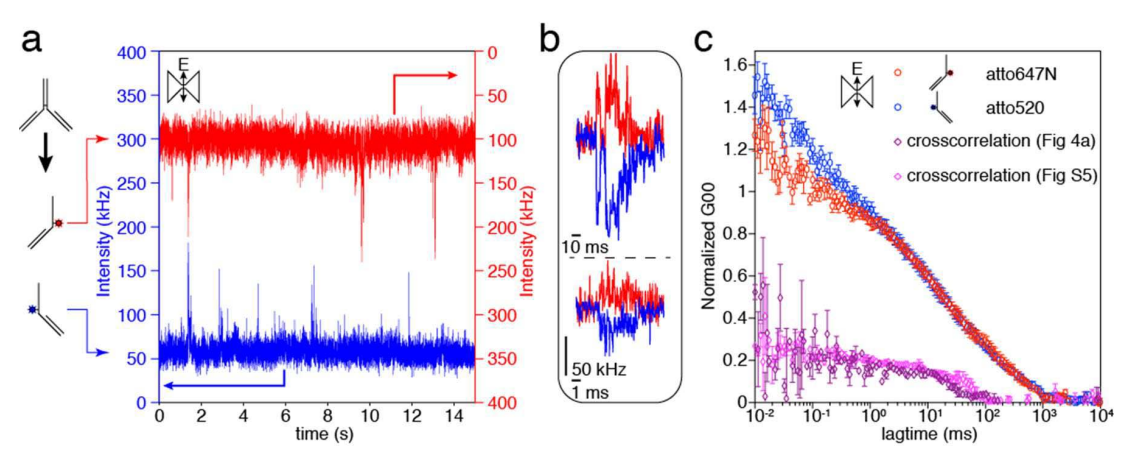


Figure 29: Simultaneous detection of multi-colour DC-SIGN mobility and transient cluster formation at the nanoscale. (a) Fluorescent time trace (1 ms bin) of single atto520 and single atto647N conjugated single chain antibodies attached to the DC-SIGN receptor that is diffusing in a live cell membrane under a transversally excited BNA antenna. (b) Zoomins of the colocalized multi-colour burst in (a). (c) Normalized autocorrelation function of the simultaneously observed DC-SIGN receptor labelled with two different colours (circles in the respective colour). Normalized cross correlation functions of the two indicated fluorescent intensity traces (diamonds).

In terms of 2D antenna arrays, we have used BNA (as described in WP3, Fig. 19) as well as planar dimer-on-boxes arrays (described in WP3, Fig. 20) to record the diffusion of individual PE lipids on living cells. Fig. 30 shows a representative array containing 40.000 BNA antennas of different gap sizes with living CHO cells seeded on the BNA substrate. We investigated antennas of different sizes, going from 20nm (the smallest gap size as shown in Fig. 30c) up to 80nm gap size. FCS curves were generated and fitted to extract the characteristic transient times of PE. However, in contrast to the BNA antenna probes described in the previous section, the FCS curves could not be fitted using a single transient time, but instead we had to use a double fitting. The results are shown in Fig. 30f for different gap sizes. Interestingly, two main regions were identified in the correlation plots. A first region where the burst intensity inversely, and sharply, correlates with burst length ($\Box_{burst} < \sim 1 \text{ms}$) and corresponds to the antenna excitation region, and a second region containing a larger number of occurrences, for $\Box_{burst} > \sim 1 \text{ms}$, where the burst intensity weakly correlates with the burst length, and corresponds to residual excitation of lipids from the BNA arms.

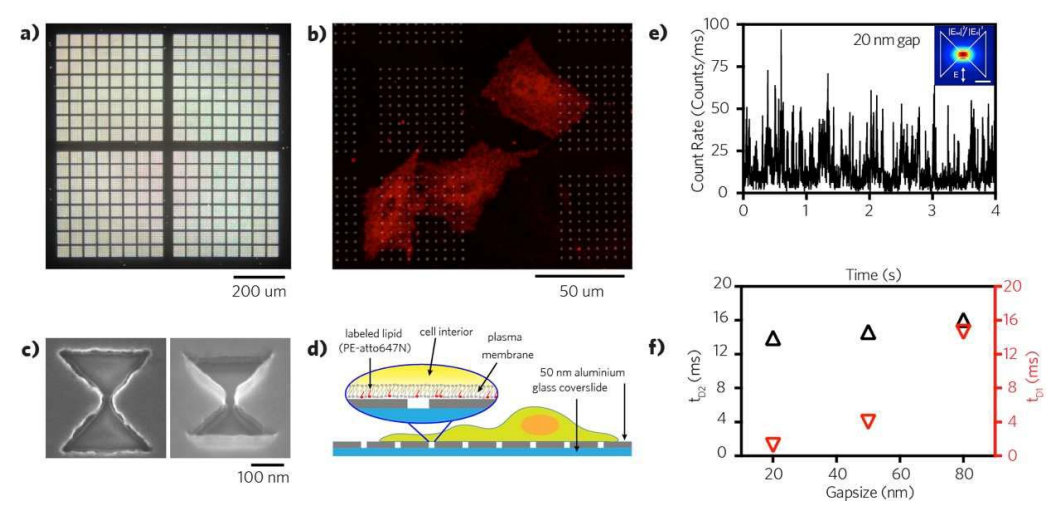


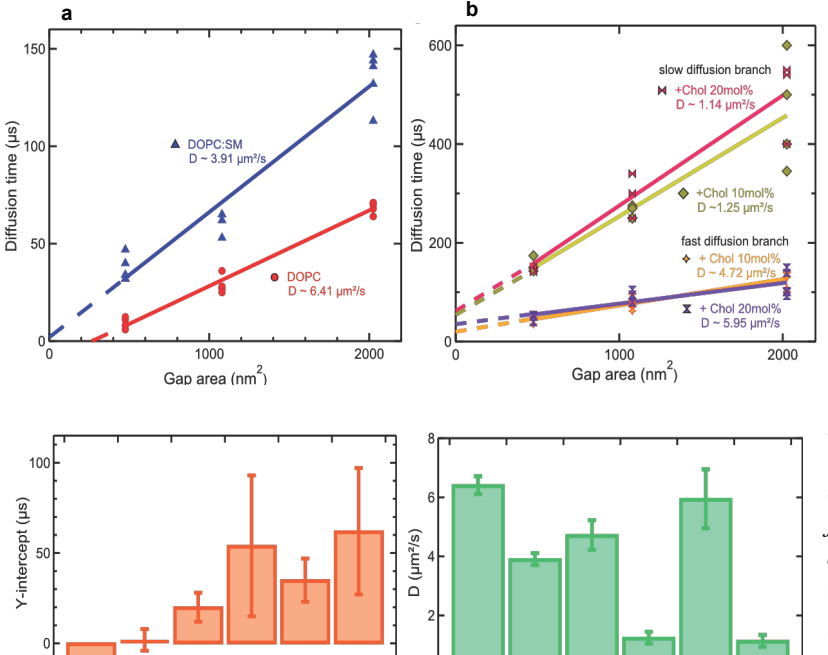
Figure 30: a) optical micrograph, in transmission illumination, of a 1x1 mm antenna array; b) detail of an antenna region with live CHO cells adhered; c) SEM micrographs of a BNA with 20 nm gap; d) schematic of the cell membrane on the antenna array; e) typical fluorescence time trace and bursts from PE-atto647N labelled lipid on a BNA with 20 nm gap; f) two component fit of autocorrelation functions from 3 different antenna gap widths. In black the constant longer contribution of the antenna arms, in red the shorter component that scales with the antenna gap in red.

Although these results were highly encouraging and we could quantitatively understand the origins for the two-components observed on the FCS curves, they also reflected the need of designing new antennas geometries in which the enhanced near-field is in closer proximity to the sample. We thus used planar antenna geometries as designed in WP3 (see Fig. 20). We assessed the performance of these antennas for individual molecules in solution (together with CNRS-IF) as well as on multicomponent lipid bilayers and living cell membranes.

For molecules in solution, and for the smallest antenna with 10 nm gap-sizes we could measure brightness up to 3000 counts/ms on single molecules having a very low quantum yield (3%) diffusing freely through the small hotspot of the antenna. This value is 1600x higher than the 0.24 counts/ms found for the dye in the confocal reference setup, and clearly demonstrates the occurrence of large fluorescence enhancement in the nanogap. Simultaneously, the fluorescence lifetime is significantly reduced from 380 ± 15 ps in confocal illumination to 45 ± 10 ps in the 10 nm gap antenna.

We also performed measurements on multi-component lipid bilayers and on living cell membranes using these planar antennas. These new devices allowed us to derive diffusion laws, by measuring the transient time of lipids for different antenna gap sizes. On multi-component lipid bilayers made of lipid DOPC, SM and different amounts of cholesterol we could reveal for the first time the

presence of nanoscopic fluctuations enriched in cholesterol as small as 14nm in size (Fig. 31 and 32). The existence of these nanoscale dynamic heterogeneities on the Lo phase has been predicted by different theoretical models but never directly observed experimentally.



Lipid bilayer composition

Figure 31: FCS diffusion laws for DOPCand DOPC:SM (a) DOPC:SM:Cholesterol *(b)* lipid mixtures. The continuous lines correspond to the fitting to the experimental data. Dash-lines are extrapolations to the y-axis to extract the t_0 values. Fitting of the slopes to straight lines renders the effective diffusion coefficient of DiD in the respective multicomponent bilayer.

Figure 32: Plots of the t_0 values (y-intercept) (left) and effective diffusion coefficient (right) derived from the FCS-diffusion law plots shown in Figure 31.

We have also performed similar types of FCS diffusion law experiments on living cell membranes. Our results show that the PE lipid diffuses

randomly on the cell surface, consistent with previous reports. Moreover, SM showed slow and anomalous diffusion, consistent with its association to cholesterol enriched nano-domains. Removal of cholesterol using the drug MCD returned a diffusion of SM close to that of PE, both in terms of diffusion coefficient values and being completely unhindered. These results thus demonstrate the validity and usefulness of antennas of different sizes and reveal the existence of cholesterol-enriched nano-domains on both multicomponent lipid bilayers and living cell membranes.

DOPC DOPC:SM Chol 10% Chol 10% Chol 20% Chol 20%

Lipid bilaver composition

Workpackage 6: Generation of a biomolecular toolbox and functional consequences in cell response: health versus disease.

According to the original proposal, the main aim of this WP has been to provide the biological support and drive to the project in terms of its biological and medical relevance. For this, we have defined two main objectives: 1) to provide the biological toolbox and suitable protocols for live cell imaging; and b) to take advantage of the antenna devices developed in NANO-VISTA to address the underlying hypothesis that the precise cell membrane nano-environment in which the cell adhesion receptor LFA-1 engages a set of effector proteins governs the ultimate signal output.

Results regarding the generation of the biological toolbox and protocols for live cell imaging.

During the course of the project we have optimized several protocols for efficient isolation of different leukocytes from human blood using buffy coats as well as protocols to generate monocytes derived dendritic cells (DC) from peripheral blood mononuclear cells (PBMC). Moreover, we have optimized different protocols for manipulating the cell lipid nano-environment as well as the actin cytoskeleton integrity of leukocytes and several cell lines. In terms of autofluorescence constructs we have now available the plasmid constructs for the following XFP-conjugated proteins: alpha L- and beta 2-chain of LFA-1, talin, vinculin, actin and tetraspanin CD81 as well as a plasmid encoding for

a GPI-anchored GFP that can be used as general GPI-anchored protein marker. All these proteins can be stably transfected in immortalized cell lines including leukocyte cell lines like RAW macrophages, THP-1 monocytes/macrophages, Jurkat T cells, K562 cells. Although stable transfection is possible, we often rely on transient transfections that we successfully perform with primary human leukocytes such as primary blood monocytes and dendritic cells. All these protocols have been sent to all the partners in the consortium and in particular, have been extensively used by ICFO partner (SMB group) and RUNMC as part of WP5 and WP6.

Results regarding studies of the cell adhesion receptor LFA-1 and effect of cell membrane nano-environment regulating LFA-1 function.

Previous results from ICFO partner (Garcia-Parajo) and RUNMC (Cambi) showed that the adhesion properties of the integrin receptor LFA-1 on leukocytes (monocytes and dendritic cells) are greatly affected by the nanoscale membrane environment of the receptor (PNAS 2009, PNAS 2012). In particular, we discovered that glyco-proteins such GPI-APs (known to control signalling) do not directly associate with LFA-1 in basal conditions. Notably, activation of LFA-1 by its ligand caused a recruitment of GPI-APs in regions of ligand-induced LFA-1 activation. Since many tumour cells show altered adhesion and migration properties we hypothesised that on these malignant cells probably the membrane environment that LFA-1 experiences might be different, which had been the initial focus of the task when writing the NANO-VISTA project. Yet, in the course of the project we realized that since GPI-APs partitions in cholesterol-enriched nanodomains, most probably the local lipid composition, presence of cholesterol and interaction with the actin cytoskeleton might influence LFA-1 organization and adhesive function. In fact, recent research indicates that the cellular levels of (glyco)-sphingolipids and cholesterol as well as the expression of lipid metabolizing enzymes are altered in a variety of diseases including cancer in response to external stimuli such as pathogens or induced by drug treatment. For example, modification of PM lipids by sphingomyelinase (SMase) is highly relevant in vivo, as triggering of human dendritic cells by Measle virus induces activation of SMase that locally alters the PM and further promotes virus uptake in these cells. SMase induces breakdown of SM into Ceramide (Cer), which partially displaces cholesterol from rafts and leads to the formation of large Cer-enriched membrane domains in model membranes. Importantly, formation and dynamics of Cer-enriched membrane platforms has been also documented in living cells, where they can influence function and avidity state of several receptors. Finally, treatment with platinumderived chemotherapeutic agents can also induce activation of SMase and subsequent alterations of SM membrane levels.

With this new interest in mind we then decided to compare LFA-1 spatiotemporal behaviour on resting monocytes and on cells with altered sphingolipid (SM) metabolism, in order to mimic a disease state. Briefly, we treated the monocytes in such a way that their cellular levels of sphingolipids and cholesterol would be altered. Since we had optimized the SMase treatment to lower SM levels, we decided to mimic what happens if the leukocytes are stimulated with platinum-based chemotherapy.

Fig. 33 shows that metabolic reduction of SM using either SMase or myriocin compromises monocyte adhesion to ICAM-1-Fc-coated fluorescent beads. Around 40% of unperturbed monocytes spontaneously bound ICAM-1, and this interaction was specifically mediated by LFA-1, as shown by the effective blocking in the presence of an anti- α_L mAb. In contrast, conversion of SM into Cer by SMase addition reduced the binding to ICAM-1 to less than 20%, as effectively as the blocking mAb. Similar to SMase, myriocin reduced the binding to ICAM-1 with respect to unperturbed cells. Thus, these results demonstrate that lipid composition regulates LFA-1 adhesive properties.

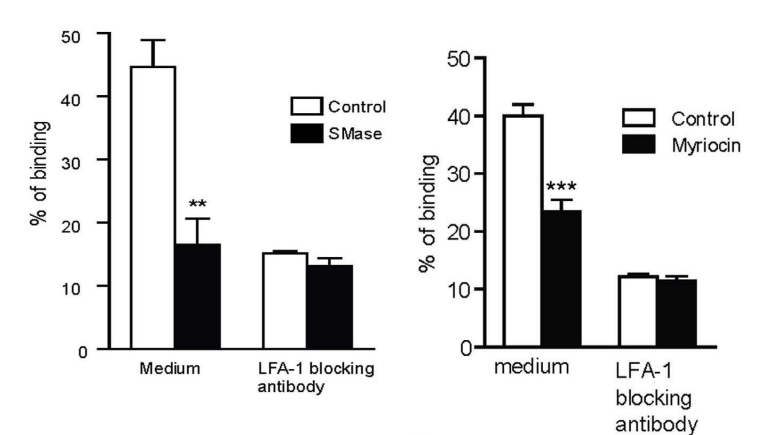


Figure 33: Monocyte adhesion to ICAM-1-Fc-coated fluorescent beads at 37°C in unperturbed and SMase, 0.05 U/ml (left) and myriocin (right) treated cells. The % of adhesion represents the amount of cells that have bound beads as determined by flow cytometry. NKI-L15 mAb was used to block LFA-1. The data show one representative experiment of 4 separate experiments. Differences were assessed by Iway ANOVA test, ***< 0.001.

Since SMase treatment decreased the overall content of SM with a

concomitant increase of Cer production at the plasma membrane, we sought to investigate how changes in the lipid nano-environment as those induced by SMase affect LFA-1 lateral mobility by exploiting FRAP and SPT approaches. By means of SPT we collected individual trajectories of diffusing LFA-1 in unperturbed monocytes and on cells treated with SMase (Fig. 34). We also performed similar experiments using myriocin (data not shown). A clear reduction of LFA-1 mobility was observed in the case of SMase treated cells (Fig. 34) while no changes in mobility were observed upon myriocin treatment. Thus, overall, our results indicate that the metabolic reduction of SM and other glycosphingolipids by myriocin as well as the patho-physiological activation of SMase with subsequent conversion of SM into Cer impact on LFA-1 function. The underlying molecular mechanisms are probably different, as Cer formation (but not myriocin) significantly hampers LFA-1 mobility.

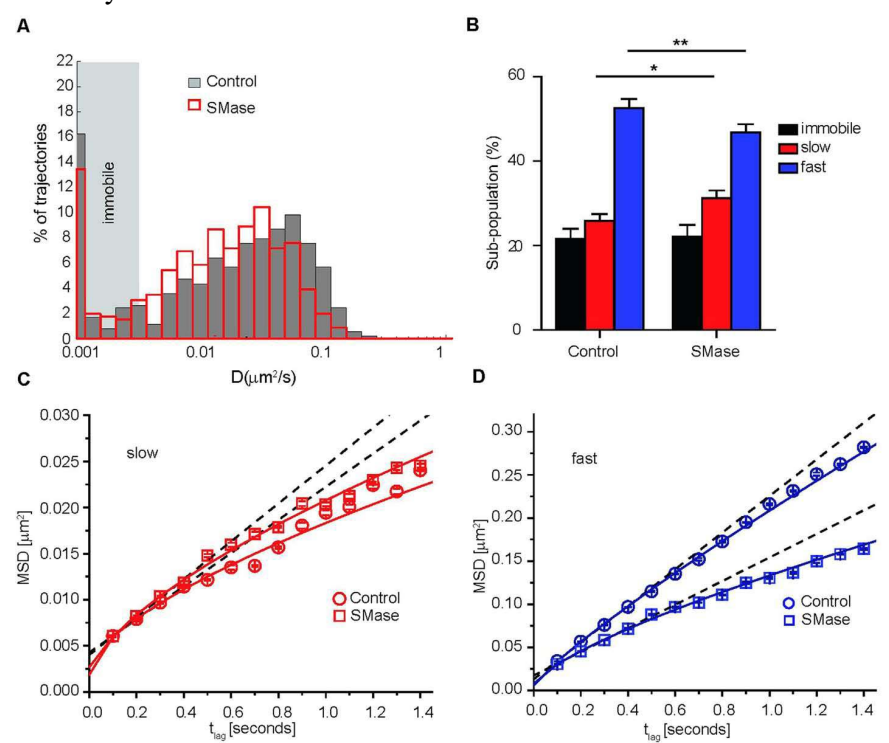
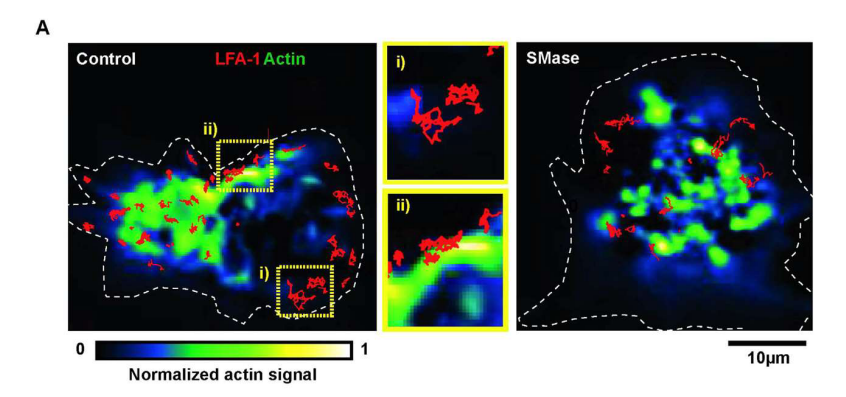


Figure 34: SMase influences the mobility lateral of LFA-1 nanoclusters (A) Normalized semilog distribution of D1-4 values for LFA-1 nanoclusters in unperturbed control cells (grey) or after SMase (red) treatment. Percentage of LFA-1 nanocluster mobility classified as immobile, slow and fast mobile in unperturbed and SMase treated monocytes. (C,D)Square displacement plots of the slow (C) and fast (D) moving population of LFA-1 by fitting the CPD at different time lags (461-658 trajectories). Slowand fast diffusing components were fitted to a model of i) free (dashed lines) and ii) anomalous diffusion (continuous lines).

It has been reported that Cer formation interferes with the dynamic organization of

the actin cytoskeleton. Since we observed a reduction in LFA-1 mobility upon Cer formation, and integrins are known to interact with the cytoskeleton, we sought to measure the mobility of individual LFA-1 nanoclusters after SMase treatment together with imaging the actin cytoskeleton in TIRF mode (Fig. 35A).



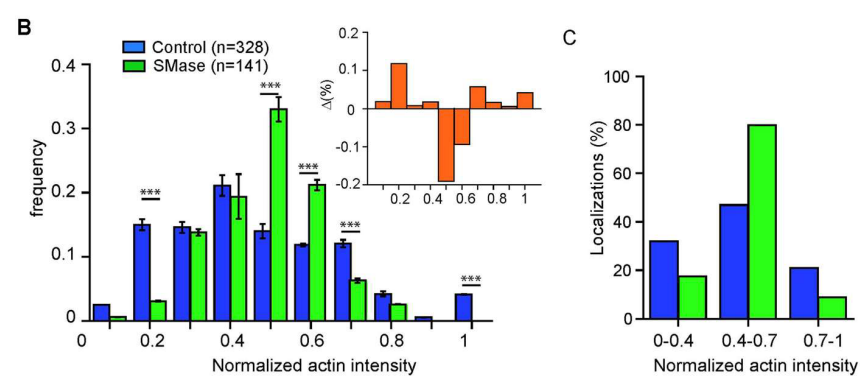


Figure 35: Increased association of LFA-1 with the cytoskeleton upon Cer formation. (A) Dual colour images of lifeact-GFP transfected monocytes and SPT of LFA-1 nanoclusters (red trajectories) in control (left) and SMase (right) cells. Custom-written software was employed to quantify and normalize the actin signal in each cell by assigning the lowest actin intensity to 0 (blue) and the highest to 1 (yellow), as indicated in the color code (bottom). White dotted lines represent the cell boundaries. Within the control cell, selected area i) represents an example of a low actin signal, while selected area ii) is an example of a high actin signal in control cells, withsuperimposed corresponding LFA-1 trajectories (red). Both selected areas are shown as enlarged images next to the control cell. (B) Distribution of normalized actin associated with

trajectory in unperturbed (blue) or SMase treated cells (green). The inset shows the difference between the normalized frequency of localizations of LFA-1 trajectories in unperturbed cells and upon SMase treatment as function of the normalized actin signal. (C) Total percentages of LFA-1 trajectory localizations in unperturbed (blue) and SMase treated cells (green) associated with the normalized actin-GFP fluorescent signal for values < 0.4, 0.4-0.7 and > 0.7 as extracted from B.

By performing dual colour SPT of LFA-1 and the actin cytoskeleton we discovered an increased association of LFA-1 with the cytoskeleton upon Cer formation. Indeed, in unperturbed cells we found that ~36% of LFA-1 trajectories preferentially localized to actin-low areas (actin index 0.1–0.4) and 46% to intermediate actin-intensities (0.4–0.6), and only a small fraction (~20%) colocalized with actin-rich areas (0.7–1) (Fig. 35B,C). In strong contrast, on SMase treated cells, a large percentage (80%) of LFA-1 trajectories were found on intermediate actin intensities. These enriched actin regions would then increase the interaction of LFA-1 with the actin cytoskeleton hindering its mobility and explaining therefore the reduction of LFA-1 mobility and its increased anomalous diffusion after SMase treatment.

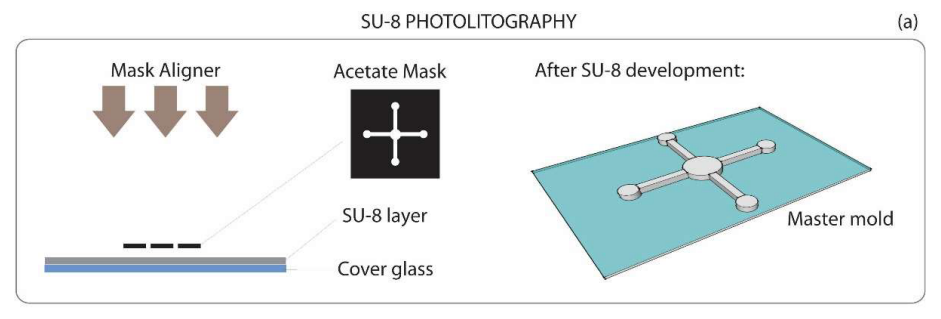
In summary, our data showed that impaired leukocyte adhesion is likely caused by altered interaction of LFA-1 with the cytoskeleton and a reduction in LFA-1 mobility upon Cer production. Such changes likely affect the adhesive properties of immune cells, which can ultimately impact on the immune response.

Workpackage 9: Development of a proto-type instrument exploiting 2D antennas in a microfluidic environment combined with single molecule fluorescence detection.

According to the original proposal, this WP has been targeted to the development of a compact, robust and highly sensitive instrument for nanospectroscopy on living cells using photonic antenna concepts. Two main objectives have been defined in this WP: 1) the development of a Lab-on-chip based on 2D antennas and microfluidic environment; and 2) the development and validation of a standalone FCS detection platform designed to work with 2D antenna arrays.

Results regarding the development of a Lab-on-chip based on 2D antennas and microfluidic environment.

Microfluidic chips have been produced by standard soft-lithography techniques and molding methods (summarized in Fig. 36). The first step is to print the designs on an acetate film. These films are used as a mask during the photolithography process to transfer the microfluidic pattern to the master mold. After that, the master mold has been fabricated by photolithography. Briefly, in this procedure, a thin layer of a negative photo-resist (SU-8 2000, Micro Chem) is first spin-coated on a coverslip and then is exposed to UV through the acetate mask. Then the substrate is developed to dissolve the unexposed regions. The resulting substrate serves as a master for fabricating PDMS molds. Master molds have been silanized to extend their lifetime.



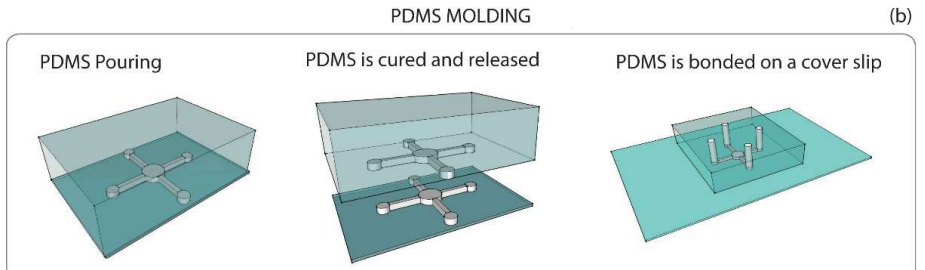


Figure 36: Chips have been done by standard SU-8 lithography and PDMS molding.

After that, the master molds are placed in a dish. Then, petri mixture 1:10 of curing agent is poured inside the petri dish and it is cured at 90 °C during 120 minutes. Once **PDMS** becomes hardened it can be released from the master mold. Inlets and outlets are then drilled onto the PDMS chip for tubing

connectors using a biopsy puncher (diameter 0.75 mm). Finally, PDMS replicas are bonded on a cover slip by plasma bonding. All steps of the microfluidic chip fabrication have been done in a clean room. In order to validate the designs and the fabrication protocol, the master molds and the PDMS chips have been characterized by means of a profilometer and an interferometric microscope. Both analyses reveal that the channel height is, as expected, around $100~\mu m$. In addition, the data acquired by means of the interferometric microscope show that the microfluidic channels of all chips present a square profile.

In our design, the PDMS chips are mounted on a custom designed micro-incubator as shown in Fig. 37 in order to keep cells at 37 degrees. The micro-incubator consists of two parts: a) a plastic chip holder that supports the microfluidic chip. This part can be easily adapted to any microscope stage and presents an aperture to enable optical access to the sample. It also ensures thermal insulation, avoiding the heat dissipates to the (metallic) platform of the microscope; and b) a metallic heater that fits into the chip holder and immobilizes the microfluidic chip. The heater provides the required temperature to the incubator by two means: direct glass substrate heating by contact and atmosphere heating by dissipation. The temperature control of the micro-incubator is achieved thanks to a closed loop using a thermistor and a pair of resistances that measure and heat the sample respectively. All the parameters are controlled and monitored by software. Liquid handling processes of the microchip are controlled and automated by means of an OEM syringe pump module that mainly consists of a syringe pump and a distribution valve. The module includes its electronic control (power supply and the specific driver for each valve). The core of the module is a 250 µl syringe pump. The syringe allows setting the speed and the direction of the pumped liquid. Our syringe pump enables flow rates

ranging from 9.7 ml/min down to 0.08 µl/min, being compatible with the protocols required for cell culturing. The integrated valve of the syringe pump has three connectors. In our design one is connected to a reservoir containing deionized water (port 1), a second one that connects the pump with the waste flask (port 2), and finally a third one that will be attached to the distribution valve of the module (port 3). This distribution valve (6 ports) that allows connecting and dispensing different samples to the PDMS chip. All ports are connected by means of Tygon tubing (internal diameter of 1/16"). Between the syringe pump and the distribution valve, a tube acts as a buffer and has to be long enough in order to avoid mixing of different liquids inside it. Syringe module is directly connected to the computer through the USB port (thanks to a RS-232 to USB converter).

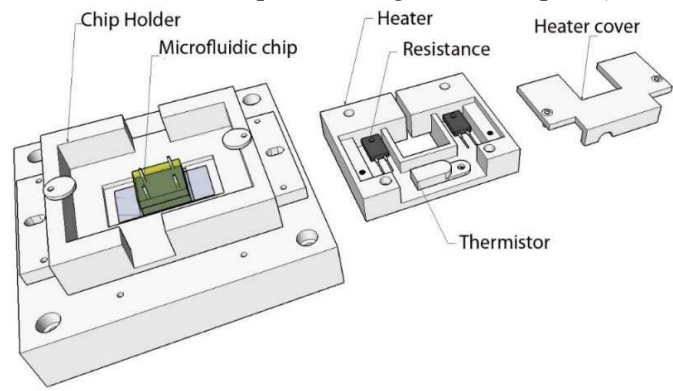


Figure 37: Design of the custom-made micro-incubator parts.

To validate the entire Lab-on-chip device together with the micro-incubator we cultured CHO cells inside the PDMS microfluidic chip (Fig. 38). Cells were placed inside the culture chamber manually and they were completely attached on the cover-glass for less than an hour. After that, the chip was placed inside a standard incubator. Cells were monitored

during 5 days and, during this period cells exhibit a proper growth and development, demonstrating that these PDMS chips are fully compatible with live cell experiments.



Figure 38: CHO cells were cultured during 5 days inside a PDMS, where cells differentiated and spread normally.

Results regarding the development and validation of a standalone FCS detection platform designed to work with 2D antenna arrays

The standalone FCS microscope was specifically conceived to excite and detect the light coming from different antennas by combining an array of photon counters (SPAD) and a spatial light modulator (SLM) (Fig. 39). An SLM was used to split up the excitation laser beam into eight independent beams that focus on a line of eight nanoantennas. The emission signal coming from the excited antennas is filtered appropriately, collected and projected on the SPAD array for the analysis in such a way that each detector collects the light coming for its respective single nanoantenna. Using this approach, the system is capable of performing FCS measurements on eight antennas at the same time. Moreover, the SLM can be used to dynamically place the laser on a particular antenna for the FCS analysis. Using this scheme we could interrogate a matrix of 8 x 8 nanoantennas without moving the sample.

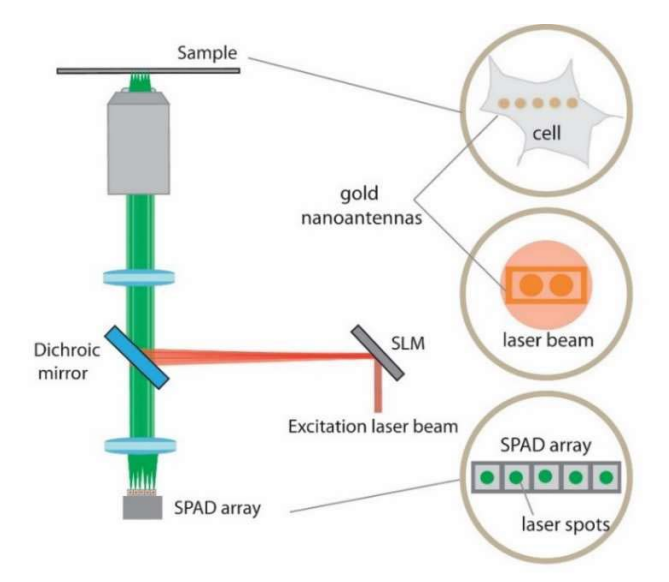


Figure 39. Sketch representing the combination of a SLM and a SPAD array detector. (a) Excitation (red) and emission (green) optical paths. For the sake of clarity, only 5 ROIs are represented in the sample, corresponding to 5 detectors of the SPAD array, and all needed lenses are not represented.

The FCS instrument is based on the optical system outlined in Fig. 40. In order extend the compatibility of the FCS instrument as much as possible the system is mounted through the lateral port of an inverted microscope. The excitation source of a He-Ne laser beam is sent to an optical fibre that is collimated and then reflected on the SLM (X11840, Hamamatsu). The proper

modulation of the polarized beam is ensured by means of a half wave plate (HWP) that allows orienting the polarization of the beam respect to the axis of the SLM. After that, the beam enters into the microscope through its lateral port and, finally, it is focused on the sample plane throughout a high numerical aperture microscope objective (60x 1.25 N.A, Nikon). The emitted light from the sample plane is collected by the same objective and transmitted through a dichroic mirror. The beam diameter is unmagnified by means of the cylindrical telescope, and, finally, it is focused on the SPAD array through an air objective. In order to facilitate the alignment process of the instrument, we have designed and produced two new custom mounts for the SPAD and the SLM. Both devices can be accurately moved through the different axis. In addition, the SLM mount enables to precisely control the orientation of the display.

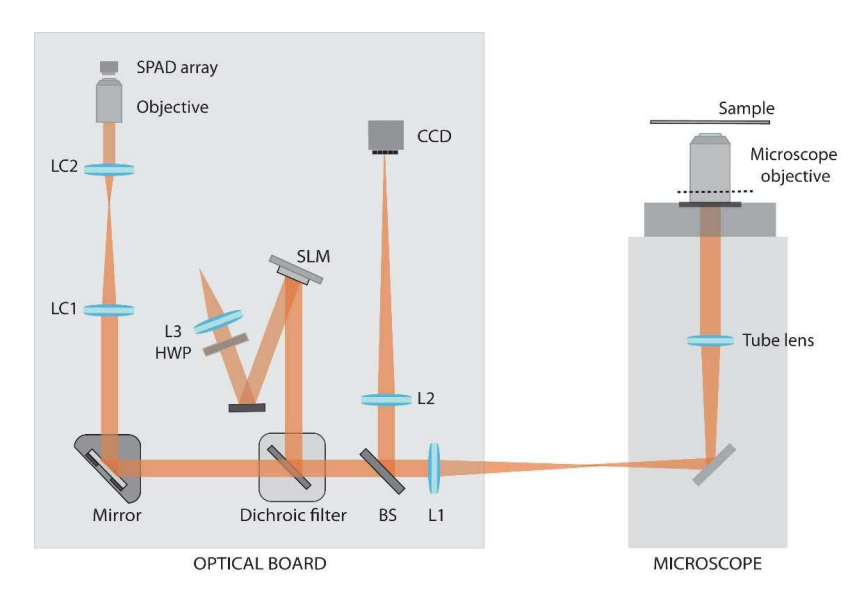


Figure 40. Optical system combining a SLM and an array of detectors SPAD to perform high throughput FCS.

Fig. 41 shows a photograph of the real system as we have implemented. All the optical components are mounted on an optical board, which is mechanically attached to the microscope through its lateral port. We have also produced a specific arduino-based circuit to control the temperature of the

SPAD in order to reduce the dark current of the detectors as maximum as possible. We then validated the proper control of the SLM to generate multiple illumination spots in real-time and have implemented a combination of lenses and gratings and random masks algorithms to dynamically create and modify multiple illumination spots. Finally, we have included a specific method to compensate for the optical aberration of the system.

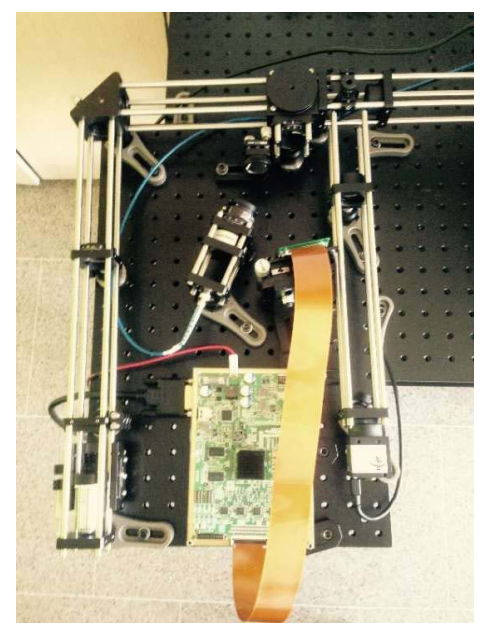




Figure 41. The setup is mounted on an optical board, which is attached to the lateral port of the microscope. During standard operation the instrument is closed using a black frame.

We have implemented all the algorithms required to process the input data. They include algorithms required to compute the histograms and the autocorrelation functions. Algorithms have been validated using artificial signals. These features allow for the calibration of the instrument, mandatory to perform the biological experiments. We have also added a specific submenu addressed to manage the fitting of the curves. We have validated it through the fitting of experimental curves acquired in collaboration with ICFO (SMB group).

In order to test the capabilities of the whole instrument, we have calibrated our system by determining its detection volume using a solution of Alexa 647 fluorescent molecules in collaboration with ICFO (SMB group). These experiments have allowed us to validate the optical system and, also, to quantitatively compare our performance respect to other commercial instruments. The preliminary conclusions indicate that the full instrument is working properly, although we still have to invest efforts on living cells, which we are currently performing in collaboration with ICFO partner (SMB group).

1.4 Potential impact of NANO-VISTA

The main aim of NANO-VISTA has been the development of a new generation of bionanophotonic tools for ultrasensitive detection, nanoimaging and nanospectroscopy of biomolecules both in-vitro and in living cells. We believe that in the future this technology will find applications in the fields of biosensing and diagnostics as well as in live cell imaging providing robust tools fully compatible with fluorescence microscopy as used in most biology research Labs. Taking advantage of the extraordinary physical properties of photonic antennas, during the course of this project we have demonstrated the generation of biophotonic-based tools with outmost performance in terms of sensitivity, selectivity and nanofocusing.

NANO-VISTA was conceived as a project that evolved from fundamental physical concepts in nanophotonics and plasmonics through technology development of different types of antenna geometries fully compatible with biological applications to the demonstration of this technology in life science applications and biosensing and finally the development of a prototype instrument for FCS measurements at the nanoscale by means of antennas. Thus, NANO-VISTA has impacted

different areas of science and technology and in the future, we expect that the impact of the project should go far beyond that of scientific knowledge generation, as discussed below.

Impact on the generation of fundamental acknowledge in nanophotonics and plasmonics:

From the fundamental point-of-view NANO-VISTA has contributed to deepen our understanding in optical local field phenomena and the physics of optical antennas. Within WP1 and WP2, ICFO and CNRS partners have developed a large variety of antenna geometries and have demonstrated their unique physical properties. For instance, CRNS has demonstrated directional control and antenna mediated spectral selection. These antennas will be interesting for future applications in the optical field in general, since it will essentially mean that in the first case (directionality) low NA objectives could be sufficient for high efficiency detection, and in the second case, direct spectral detection would be possible without the requirement of fluorescent filters. Thus, applications far beyond those explored in this project are foreseeable. These type of "devices" could, for instance, develop into European marketable products, in the mid-long run. Moreover, CNRS has exploited the huge local field enhancement to burst the fluorescence emission of weakly fluorescing molecules including light harvesting systems. This unique property means that antenna devices could be used to increase the fluorescence of many organic molecules or autofluorescent proteins that commonly suffer from low quantum yield.

Fluorescence single molecule sensors based on plasmonic metal nanostructures are currently limited by the non-radiative energy transfer between emitters and free electron gas and by the Joule heating caused by the excitation laser beam. A new paradigm is needed to design optical antennas without these limitations so as to implement reliable and cost effective molecular sensors with on-chip and CMOS compatible nanophotonic devices. Silicon-based nanophotonics is currently one of the very active approaches to meet this goal. Within NANO-VISTA, CNRS partner has reported the first all-dielectric nanoantennas able to enhance the fluorescence signal of individual molecules at biological concentrations. We have designed and fabricated all-silicon nanogap antennas that confine light by 3600-fold below the diffraction limited confocal volume and provide fluorescence enhancement up to 270×. This gives the first experimental evidence that silicon nanoantennas can achieve fluorescence enhancements above 200-fold and allow the detection of individual molecules at micromolar concentration using dielectric materials only. These results open new routes to implement high sensitivity molecular (bio)sensors with on-chip photonic devices that are CMOS compatible.

Confining light at a spatial scale comparable to the molecular size also opens new opportunities to enhance Förster resonance energy transfer (FRET), which is a ubiquitous phenomenon governing the energy exchange at the nanoscale and is widely applied in biochemistry, organic photovoltaics, and lighting sources. However, earlier FRET experiments exploiting simple photonic structures (mirrors, microcavities, dielectric particles) did not offer the full potential of resonant plasmonic antennas. Within NANO-VISTA, CNRS and ICFO partners have introduced a resonant nanogap antenna tailored to enhance single molecule FRET. Our single-molecule experiments have reported a 10-fold increase in the photonic density of states together with an unprecedented 5-fold enhancement of the FRET rate. Importantly for practical applications, our work has demonstrated that optical antennas can extend the spatial range of FRET to distances where dipole-dipole interactions would otherwise be too weak to produce detectable FRET signals. Moreover, we have introduced clear design rules to enhance the FRET rate with a nanoantenna. This understanding is essential for the future development of nanophotonics to control energy transfer on nanometre distances for applications in photovoltaics, organic lighting sources and biosensing.

FRET is highly sensitive to the mutual orientation of donor and acceptor dipoles, and is strongly prohibited for perpendicularly oriented dipoles. This orientation dependence is a major obstacle for the FRET analysis, especially on protein samples where the mobility of the fluorophores is often

constrained. Within NANO-VISTA, ICFO and CNRS partners have shown a novel use of plasmonic nanoantennas to exploit the orientation dependence in FRET in our advantage. We have demonstrated that the nanoantenna creates favourable conditions for the donor dipole radiation, generating strongly inhomogeneous and localized fields in the nanogap, which open new energy transfer routes, overcome the limitations from the mutual dipole orientation, and ultimately enhance the FRET efficiency. While several previous works on FRET with nanophotonic structures addressed the link between FRET and the local density of optical states (LDOS), our work has been the first to bridge the gap between FRET orientation effects and near-field optics, showing that FRET is allowed in the nanoantenna even for perpendicularly oriented donor and acceptor pairs. Our findings provide a new strategy to use nanophotonics to reveal FRET interactions that would otherwise be impossible to probe using diffraction-limited microscopes. This non-explored aspect of nanoantennas has wide applications for various communities, from fundamental near-field optics to bioapplications of single-molecule FRET.

Impact on the generation of new technologies:

One of the strongest bottlenecks that have prevented wide spread of near-field scanning optical microscopy (NSOM) in the scientific community is the limited light throughput of conventional NSOM probes. Indeed, there is a compromise in terms of the size of the subwavelength apertures used for NSOM, which dictate the final optical resolution to be achieved, and the power throughput, i.e., the smaller the diameter of the probe, the higher the resolution but also the lower the power throughput. Therefore for practical applications, most NSOM probes have a final diameter of 70nm or larger, which is rather modest. One of the major breakthroughs of NANO-VISTA has been the fabrication of antenna probes at the apex of tapered metal-coated optical fibres. The combination of huge field enhancement (typically 3 orders of magnitude higher as compared to conventional NSOM probes) and the nanofocussing of antennas have allowed us to demonstrate 20nm true optical resolution together with sub-nanometre localization accuracy on individual molecules which is unique in the world. The extraordinary performance of these antenna probes as compared to those currently available in the market has raised interest from several companies that manufacture scanning probe microscopes. In particular, ICFO has pioneered a project in collaboration with the Company WITec with the aim of fabricating bowtie antennas at the apex of their commercial hollow cantilevers. Using a demo system from WITec we demonstrated 40nm optical resolution by means of these engineered antennas. Currently, ICFO (SMB group) is in discussions with WITec for future developments and technology transfer of the antennas. We believe that an enormous potential exists for the generation of new products based on antenna probes by European Industries, and applications beyond those addressed in this project. Indeed, NSOM is a microscopy technique used in physics, materials and Biotech. Labs.

Another major asset in the project has been the fabrication of large substrate areas covered by nano-antennas in order to render them compatible with Life Science applications. We have dedicated a full workpackage (WP3) to this part since it is crucial for any realistic application in the cell biology field: biological experiments require lengthy essays with many cells and multiple repetitions to confirm reproducibility and to deal with cell variability. Within NANO-VISTA, EPFL partner has devised new nano-fabrication methods to produce low-cost, large arrays of 2D antennas with high reproducibility and have pioneered their application for biosensing and live cell research. For instance, EPFL, ICFO and CNRS partners have shown detection of individual DNA molecules at concentrations in the micromolar range, which is four to five orders of magnitude higher than standard confocal detection. Moreover, the same partners have shown for the first time the detection of individual nanodomains and nanoscopic cholesterol-dependent fluctuations on multicomponent lipid bilayers and living cells. These results demonstrate the outstanding performance of these antenna devices and should open up new research in biotechnology and biophysics. The partner responsible for WP3 is at EPFL, a high education centre that strongly encourages and supports

technology transfer and creation of spin-offs. Within NANO-VISTA we have explored the possibility of transferring these nano-fabrication methodologies to an EPFL spin-off company. Currently, the market is still too small given the fact that the community is not ready yet to take up these concepts into future devices. Nevertheless, in the future one can envisage the rapid, cost-efficient large scale-fabrication of antenna substrates for biosensing, imaging and live cell spectroscopy at the nanometre scale fully compatible with standard fluorescence microscopes. In the long run these substrates could be commercialised as "kit-antenna substrates" for dedicated biological experiments at the nanometre scale and on living cells, a long-awaiting dream of cell biologists. Along these lines, one of the major manufacturers of single molecule FCS instruments (PicoQuant) has shown genuine interest in these devices to be coupled to their standard single-molecule MicroTime system increasing the power of their instrument to achieve single molecule detection at physiological concentration levels.

Impact in European Science and Technology development and visibility:

As a true interdisciplinary project, NANO-VISTA has expanded the knowledge and know-how technology at the European level in multiple fields of science and technology, including nanophotonics, plasmonics nanofabrication, single molecule detection, biophysics and cell biology amongst others. The major breakthroughs in terms of fundamental research and technology development mentioned above have been worldwide spread and we can honestly say that we have provided outstanding visibility to European research. This is manifested by the large number of invited talks and seminars worldwide delivered by members of this consortium (see below). Moreover, within NANO-VISTA we have also produced three different Newsletters where we have disseminated the most important results of the project making the international community aware of the project and the most novel advances in European research.

The NANO-VISTA consortium was composed by six partners from four different European countries. The large scope of the project spanning fundamental, technological and biological fields has required to set-up a multi-disciplinary team of experts from different institutions and complementary backgrounds that it is difficult to find in only one country. This joint venture has served to re-enforce European research, so that we have all benefited from mutual collaborations and have opened new research avenues. For instance, NANO-VISTA has served to increase the visibility of Spanish research in the fields of nanophotonics and plasmonics, which has been lacking behind compared to other European countries. This has contributed to the generation of new funded national research projects to the groups of Garcia-Parajo and van Hulst, both members of the consortium at ICFO. Another example is given by the group of EPFL, which has been very well known in the field of micro- and nanofabrication and now, thanks to NANO-VISTA, is becoming a leader research group in the field of plasmonic applications for biosensing and biology. In summary, NANO-VISTA has brought the opportunity to further improve scientific and technological cooperation for benefits of all partners, strengthening in turn the trans-national European research cohesion. Most importantly, the manifold of European contacts held by the different partners has allowed the distribution of knowledge amongst the most application-oriented research community active in the

Societal impact of NANO-VISTA

NANO-VISTA belongs to the kind of visionary projects aimed to develop photonic disruptive technologies for future applications in the fields of biosensing and live cell research. As such, the true impact in Society is still to come. Nevertheless, during the whole duration of the project we have paid most attention to disseminate the results of NANO-VISTA to the general public through TV interviews, general talks designed to a broad audience, open days in each of the Institutions participating in the consortium, Newsletters and magazines. In this way, we have tried to reach the general public making them aware of the research and technological developments in Europe.

In terms of training the new generation of scientists and technologists in Europe, NANO-VISTA has been extremely successful. During the course of the project, six different PhD theses have been defended and two more are to be defended in 2017. All these new professionals have already found PostDoctoral positions at leading research Institutes worldwide (Harvard, MIT, CalTec, Delft University, Eindhoven Technical University, etc) or in industry.

In terms of exploitation of NANO-VISTA results for the generation of a new industrial sector, we have filed two patents during the project (from CNRS) and a third one from COSINGO is currently in progress (preliminary patent search and FTO, invention disclosure filled). Moreover, we explored transferability of know-how on 2D antenna geometries to the start-up company micro-litho (EPFL) and have established strong links with the Microscopy Companies PicoQuant (CNRS & ICFO) and WiTec (ICFO). We feel that the first-step on this core technology is now ready and mature but major efforts would have still to be invested before transferring these devices into commercial market products.

In summary, with the innovative elements brought about by this project, well beyond the current state-of-art, we have produced a technological breakthrough in Europe. We have furthered scientific progress in the booming fields of nanophotonics and plasmonics, and nanofabrication technologies for large -scale integration far beyond those related to life sciences. We believe that in the future this technology should open the way to the development of new biophotonic tools that in the long term could result in market products in sector areas of biosensing and/or biology research Labs.

Main dissemination activities of NANO-VISTA and exploitation of results

The research being performed during NANO-VISTA has led to a total of 42 papers in the most influential journals in the field, including Nature Nanotechnology (2), Nature Communications (1), Nano Letters (13), Nano Today, PNAS, Phys. Rev. Lett, etc. Moreover, partners of this consortium have delivered a total of 212 contributions at major conferences, workshops and seminars at different research institutions around the world (including 132 invited talks from the PIs involved in the project). Importantly in terms of nurturing new research scientists in the field, NANO-VISTA has produced eight PhD research theses. These impressive numbers highlight the success of NANO-VISTA and the enormous impact that the project has had in the international scientific community.

In terms of exploitation of NANO-VISTA results for the generation of a new industrial sector, we have filed two patents during the project and a third one is currently in progress (preliminary patent search and FTO, invention disclosure filled). Moreover, we explored transferability of know-how on 2D antenna geometries to the start-up company micro-litho and have established strong links with the Microscopy Companies PicoQuant and WiTec. We feel that the first-step on this core technology is now ready and mature but major efforts would have still to be invested before transferring these devices into commercial market products.

Below we summarize the main dissemination activities of NANO-VISTA, separated in terms of scientific, peer-review publications, invited oral contributions (only the most salient ones), talks targeted to the broad audience together with news from highlights of the most prominent results and European networking activities.

Peer-review publications:

- 1. V. Flauraud, M. Mastrangeli, G. D. Bernasconi, J. Butet, D. Alexander, E. Shahrabi, O. Martin and <u>J. Brugger</u>. Nanoscale topographical control of capillary assembly of nanoparticles, *Nature Nanotechnology* doi:10.1038/nnano.2016.179 (2016).
- 2. V. Flauraud, R. Regmi, P. M. Winkler, D. T. L. Alexander, <u>H. Rigneault, N. F. van Hulst, M. F. Garcia-Parajo, J. Wenger, J. Brugger</u>. Turning Plasmonic Antennas on the Right Side: Template Stripping Maximizes Single Molecule Fluorescence Enhancement, *Nano Letters*, under review.

- 3. P. M. Winkler, R. Regmi, V. Flauraud, <u>J. Brugger, H. Rigneault, J. Wenger, M. F. Garcia-Parajo</u>. Nanoscopic phase separation in model lipid membranes resolved by in-plane plasmonic antenna arrays, *ACS nano*, under review.
- 4. J. de Torres, M. Mivelle, S. B. Moparthi, <u>H. Rigneault, N. F. van Hulst, M. F. García-Parajó</u>, E. Margeat, <u>J. Wenger</u>, Plasmonic Nanoantennas Enable Forbidden Förster Dipole-Dipole Energy Transfer and Enhance the FRET Efficiency, *Nano Letters* **16**, 6222 (2016).
- 5. R. Regmi, J. Berthelot, P. M. Winkler, M. Mivelle, J. Proust, F. Bedu, I. Ozerov, T. Begou, J. Lumeau, H. Rigneault, M. F. García-Parajó, S. Bidault, J. Wenger, N. Bonod, All-Dielectric Silicon Nanogap Antennas To Enhance the Fluorescence of Single Molecules, *Nano Letters* 16, 5143 (2016).
- 6. F. Yesilkoy, V. Flauraud, M. Rüegg, B. J. Kim and <u>J. Brugger.</u> 3D nanostructures fabricated by advanced stencil lithography, *Nanoscale* **8**, 4945 (2016).
- 7. F. Yesilkoy, R. Ueno, B. X. E. Desbiolles, M. Grisi, Y. Sakai, B. J. Kim and <u>J. Brugger.</u> Highly efficient and gentle trapping of single cells in large microfluidic arrays for time-lapse experiments, *Biomicrofluidics* **10**, 10.1063/1.4942457 (2016).
- 8. A.-L. Le Roux, B. Castro, E. T. Garbacik, M. F. Garcia Parajo, M. Pons, Single molecule fluorescence reveals dimerization of myristoylated Src N-terminal region on supported lipid bilayers, *Chemistry Select* 1, 642 (2016).
- 9. <u>J. Wenger</u>, R. Regmi, <u>H. Rigneault</u>, Plasmonic-enhanced fluorescence detection of single molecules at high concentrations in Roadmap on biosensing and photonics with advanced nano-optical methods, edited by E. Di Fabrizio, *J. Optics* **18**, 063003 (2016).
- 10. M. F. Garcia-Parajo, Nanophotonic approaches for nanoscale imaging and nanospectroscopy in living cells in Roadmap on biosensing and photonics with advanced nano-optical methods, edited by E. Di Fabrizio, *J. Optics* **18**, 063003 (2016).
- 11. N.F. van Hulst, Optical antennas for localized and enhanced interaction with single-photon emitters in Roadmap on biosensing and photonics with advanced nano-optical methods, edited by E. Di Fabrizio, *J. Optics* **18**, 063003 (2016).
- 12. C. Eich, C. Manzo, S. de Keijzer, G.-J. Bakker, I. Reinieren-Beeren, M. F. García-Parajo, A. Cambi, Changes in membrane sphingolipid composition modulate dynamics and adhesion of integrin nanoclusters, *Sci. Rep.* **6**, 20693 (2016).
- 13. J. A. Torreno-Pina, C. Manzo, M. F. Garcia-Parajo, Uncovering homo-and hetero-interactions on the cell membrane using single particle tracking approaches. J. Phys. D Appl. Phys. 49, 104002 (2016).
- 14. J. A. Torreno-Pina, C. Manzo, M. Salio, M. C. Aichingerb, A. Oddone, M. Lakadamyali, D. Shepherd, G. S. Besra, E. V. Cerundolo M. F. Garcia-Parajo, The actin cytoskeleton modulates the activation of iNKT cells by segregating CD1d nanoclusters on antigen-presenting cells *P. Natl. Acad. Sci. USA* 113, E772–E781 (2016).
- 15. A. Singh, J. T Hugall, G. Calbris, N. F. van Hulst, "Fiber-based Optical Nanoantennas for Single Molecule Imaging and Sensing", *J. Lightwave Technol.* **33**, 2371-2377 (2015).
- 16. P. Ghenuche, M. Mivelle, J. de Torres, S. Babu Moparthi, <u>H. Rigneault, N. F. van Hulst, M. F. García-Parajo</u>, <u>J.Wenger</u>, "Matching Nanoantenna Field Confinement to FRET Distances Enhances Förster Energy Transfer Rates", *Nano Letters* **15**, 6193 (2015).
- 17. Niek F. van Hulst, "Single-Molecule Microscopy and Spectroscopy: Concluding Remarks", *Faraday Discussions* (2015); DOI: 10.1039/C5FD00147A.

- 18. C. Manzo, M. F. Garcia-Parajo. A review of progress in single particle tracking: from methods to biophysical insights. *Rep. Prog. Phys.* **78**, 124601 (2015).
- 19. M. Mivelle, T. Grosjean, G. W. Burr, U. C. Fischer, M. F. Garcia-Parajo, Strong modification of magnetic dipole emission through diabolo nanoantennas *ACS Photonics* **2**, 1071 (2015).
- 20. V. Flauraud, T. S. van Zanten, M. Mivelle, C. Manzo, M. F. Garcia Parajo, J. Brugger, Large-scale arrays of bowtie nanoaperture antennas for nanoscale dynamics in living cell membranes, *Nano Letters* **15**, 4176 (2015).
- 21. C. Manzo, J. A. Torreno-Pina, P. Massignan, G. J. Lapeyre, Jr., M. Lewenstein, M. F. Garcia Parajo Weak ergodicity breaking of receptor motion in living cells stemming from random diffusivity. Phys. Rev. X 5, 011021 (2015).
- 22. R. Regmi, A. A. Al Balushi, <u>H. Rigneault</u>, R. Gordon, <u>J. Wenger</u>, Nanoscale volume confinement and fluorescence enhancement with double nanohole aperture, *Scientific Reports* **5**, 15852 (2015).
- 23. D. Punj, R. Regmi, A. Devilez, R. Plauchu, S. B. Moparthi, B. Stout, N. Bonod, <u>H. Rigneault</u>, <u>J. Wenger</u>, Self-Assembled Nanoparticle Dimer Antennas for Plasmonic-Enhanced Single-Molecule Fluorescence Detection at Micromolar Concentrations, *ACS Photonics* **2**, 1099-1107 (2015).
- 24. J.A. Torreno-Pina, B. Castro, C. Manzo, S. Buschow, <u>A. Cambi, M.F. Garcia-Parajo</u>. Enhanced receptor-clathrin interactions induced by N-glycan mediated membrane micropatterning. *Proc. Nat. Acad. Sci. USA*, **111**, 11037 (2014).
- 25. M.F. Garcia-Parajo, A. Cambi, N. Thompson, K. Jacobson. Nanoclustering as a dominant feature of plasma membrane organization. *J. Cell Sci.* **127**, 4995–5005 (2014). **Invited commentary.**
- 26. M. Mivelle, T.S. van Zanten, <u>M.F. Garcia-Parajo</u>. Hybrid photonic antennas for subnanometer multicolor localization and nanoimaging of single molecules. *Nano Letters* **14**, 4895 (2014).
- 27. A. Singh, G. Calbris, N. F. van Hulst, Vectorial nanoscale mapping of optical antenna fields by single molecule dipoles, *Nano Letters* **14**, 4715 (2014).
- 28. D. Punj, P. Ghenuche, S. B. Moparthi, J. de Torres, V. Grigoriev, <u>H. Rigneault, J. Wenger,</u> Plasmonic antennas and zero-mode waveguides to enhance single molecule fluorescence detection and fluorescence correlation spectroscopy towards physiological concentrations, *WIRE Nanomed Nanobiotechnol* **6**, 268 (2014).
- 29. K.J.E. Borgman, T.S. van Zanten, C. Manzo, R. Cabezon, <u>A. Cambi</u>, D. Benitez-Ribas, <u>M.F. Garcia-Parajo</u>. Priming by chemockines restricts lateral mobility of the adhesion receptor LFA-1 and restores adhesion to ICAM-1 nano-aggregates on human mature dendritic cells. *PLoS ONE* **9**, e99589 (2014).
- 30. M. Mivelle, T.S. van Zanten, C. Manzo, <u>M.F. Garcia-Parajo</u>. Nanophotonic approaches for nanoscale imaging and single molecule detection at ultra-high concentrations. *Microscopy Research Techniques* 77, 537 (2014) **invited review**.
- 31. P. Massignan, C. Manzo, J.A. Torreno-Pina, <u>M.F. Garcia-Parajo</u>, M. Lewenstein, G.J. Lapeyre. Nonergodic subdiffusion from Brownian motion in an inhomogeneous medium. *Phys. Rev. Lett.* **112**, 150603 (2014).
- 32. C. Manzo, T.S. van Zanten, S. Saha, J.A. Torreno-Pina, S. Mayor, <u>M.F. Garcia-Parajo</u>. PSF decomposition of nanoscopic images via Bayesian analysis unravels distinct molecular organization of the cell membrane. *Scientific Reports* 4, 4354 (2014).

- 33. D. Punj, J. de Torres, <u>H. Rigneault</u>, <u>J. Wenger</u>, Gold nanoparticles for enhanced single molecule fluorescence analysis at micromolar concentration, *Opt. Express* **21**, 27338 (2013).
- 34. Langguth L., Punj D., Wenger J., Koenderink F. Plasmonic Band Structure Controls Single-Molecule Fluorescence, ACS Nano 7, 8840 (2013).
- 35. D. Punj, M. Mivelle, S. B. Moparthi, T. S. van Zanten, <u>H. Rigneault, N. F. van Hulst, M. F. Garcia-Parajo</u>, <u>J. Wenger</u>, A plasmonic 'antenna-in-box' platform for enhanced single-molecule analysis at micromolar concentrations, *Nature Nanotechnology* **8**, 512 (2013).
- 36. Meddens MB, Rieger B, Figdor CG, <u>Cambi A</u>, van den Dries K. Automated Podosome Identification and Characterization in Fluorescence Microscopy Images. *Microsc Microanal*, 1-10 (2013).
- 37. van den Dries K, Meddens MB, de Keijzer S, Shekhar S, Subramaniam V, Figdor CG, <u>Cambi A</u>. Interplay between myosin IIA-mediated contractility and actin network integrity orchestrates podosome composition and oscillations. *Nature Commun*, **4**, 1412 (2013).
- 38. L. Neumann, J. van't Oever, Anshuman Singh, N.F. van Hulst, A Scanning Resonant Dipole Antenna Probe for enhanced nanoscale imaging. *Nano Letters* **13**, 5070 (2013).
- 39. van den Dries K, Schwartz SL, Byars J, Meddens MB, Bolomini-Vittori M, Lidke DS, Figdor CG, Lidke KA, <u>Cambi A.</u> Dual color super-resolution microscopy reveals nanoscale organization of mechanosensory podosomes. *Mol Biol Cell.* **24**, 2112 (2013).
- 40. V. Auzelyte, B. Gallinet, V. Flauraud, Ch. Santschi, S. Dutta-Gupta, O. J. F. Martin and <u>J. Brugger</u>, Large area gold/parylene plasmonic nanostructures fabricated by direct nanocutting. *Advanced Optical Materials* **1**, 50 (2012), **coverpage**.
- 41. H. Aouani, R. Hostein, O. Mahboub, E. Devaux, <u>H. Rigneault</u>, T.W. Ebbesen, and J. Wenger, Saturated excitation of fluorescence to quantify excitation enhancement in aperture antennas, *Opt. Express* **20**, 18085 (2012).
- 42. Y. F. Dufrêne, M. F. Garcia-Parajo, Recent progress in cell surface nanoscopy: Light and force in the near-field, *Nano Today* 7, 390 (2012).
- 43. M. Mivelle, T. S. van Zanten, L. Neumann, N. F. van Hulst, M. F. Garcia-Parajo Ultra-bright, free-standing bowtie nanoperture antennas probed by single molecule fluorescence, *Nano Letters* 12, 5972 (2012).

Most influential oral contributions upon invitation

- 1. M. F. Garcia-Parajo. "Optical nano-tools for multi-colour imaging and dynamics at the nanoscale". Invited speaker at the International Microscopy Mela event at NCBS, Bangalore, India. 24-25 September 2016.
- 2. <u>M. F. Garcia-Parajo.</u> "Membrane receptor nanoclustering as functional unit of immune cells". Invited speaker at the International Microscopy Workshop at NCBS, Bangalore India. 22 September 2016.
- 3. <u>M. F. Garcia-Parajo.</u> "Cell membrane heterogeneity, molecular diffusion and function". Invited speaker at the Mini-Symposium *Anomalous transport in crowded cells and soft matter*, 26th European Physical Society-Condensed Matter Division meeting, Groningen, the Netherlands. 05-09 September 2016.
- 4. M. F. Garcia-Parajo. "Protein nanoclustering as a functional unit of immune cells". Invited talk at the Symposium Chemomechanical coupling in immune response at the 60th Annual meeting of the American Biophysical Society, Los Angeles. USA. 27 February 2 March 2016.

- 5. M. F. Garcia-Parajo. "Protein nanoclustering as a functional unit of immune cells". Plenary talk at the XVIII Annual Linz Winter Workshop: Advances in Single-molecule research from Biology to Nanoscience". Linz, Austria. 29 January- 1 February 2016.
- 6. <u>M. F. Garcia-Parajo.</u> "Nanophotonics for live cell research: from nanoimaging to spectroscopy". Invited Seminar at the Cavendish Laboratory, University of Cambridge, UK. 20 Nov. 2015.
- 7. N. F. van Hulst "Optical nanoantennas for nanoscale imaging of ultrafast dynamics in single biomolecules", 2nd Microscopy Congress: Utilising Microscopical Technologies as a Tool for Progressing Medical Research, 14-15 November 2016, London, UK (United Kingdom)
- 8. <u>N. F. van Hulst</u> ""Femtosecond dynamics at the nanoscale", "Leading Light Symposium" Fom Institute AMOLF, 27 October 2016, Amsterdam, the Netherlands (The Netherlands)
- 9. N. F. van Hulst "Light at the nanoscale: ultrafast meets ultrasmall", PIER Graduate Week 2016, Interdisciplinary lectures and workshops for PhD students, 10 13 Oct 2016, CFEL, Bahrenfeld Campus, Hamburg (Germany)
- 10. N. F. van Hulst NanoPhotonics Meets Biology, Physics Meets Biology 2016, 12-14 Sept 2016, Cambridge (United Kingdom)
- 11. N. F. van Hulst "Coherent feedback control of optical antennas and single photon emitters", COST workshop WG2: Quantum Coherence on the Nanoscale, Marseille 30 May 2016 (France)
- 12. N. F. van Hulst "Nanoantennas for molecular antennas: revealing quantum responses in individual photosynthetic complexes", Colloquium at CNR-Nano Modena (Italy)
- 13. N. F. van Hulst Coherent feedback control of optical antenna systems, NanoLight 2016, 7-11 March 2016, Benasque, Aragon (Spain)
- 14. N. F. van Hulst NanoPhotonics: ultrafast control of nanoparticles, nanoantennas and single quantum emitters, NanoPT2016, 16-19 February Braga (Portugal)
- 15. N. F. van Hulst Single-Molecule Microscopy and Spectroscopy: Concluding Lecture Single-Molecule Microscopy and Spectroscopy: Faraday Discussion 184, 14-16 Sep 2015, London, UK
- 16. <u>N. F. van Hulst</u> Single-Molecule Ultrafast Photonics "Frontiers in Nanophotonics", Monte Verità, Ascona, Switzerland, 30 Aug 4 Sep 2015 (Switzerland)
- 17. N. F. van Hulst Talking to antenna complexes one-by-one: femtosecond dynamics at the nanoscale QUEBS2015, Florence, Italy, 29 June 2 July 2015 (Italy)
- 18. N. F. van Hulst Keynote speaker. Light: Pushing the Fast and the Small. CLEO-Europe, 21-25 June 2015, Munich, Germany.
- 19. N. F. van Hulst Quantum nano-optics in single light harvesting complexes DINAMO: Discussions on Nano & Mesoscopic Optics, April 8-12, 2015. El Chaltén, Patagonia, (Argentina)
- 20. N. F. van Hulst Nanoplasmonics. Plenary address. Nanoplasmonics: Faraday Discussion 178, 16-18 Feb 2015, Chem. Centre, London. United Kingdom.
- 21. N. F. van Hulst Keynote speaker, Ultrafast laser pulse control and interaction with nanostructures and molecules SPIE Photonic West, 7-12 Feb 2015, San Francisco, USA.
- 22. N. F. van Hulst Antennas for Light: Femtosecond Control on the Nanoscale Enrico Fermi Colloquium, LENS, Florence, 28 November 2014 (Italy)
- 23. N. F. van Hulst "Femtosecond control on the nanoscale". NFO-13. 13th international conference of Near-field Optics and Nanophotonics. 31 Aug 4 Sep 2014, Salt Lake City, Utah, USA.
- 24. <u>J. Brugger</u> Invited talk at MEMS and NANOTECHNOLOGY, Institute colloquium at Adophe Merkle Institute, Fribourg, Switzerland, 13 April 2016.
- 25. <u>J. Brugger</u> Nanofabrication using top-down and bottom-up techniques: recent progress to improve control, throughput and cost-efficiency, The 11th Annual IEEE International

- Conference on Nano/Micro Engineered and Molecular Systems (IEEE-NEMS 2016), Matsushima Bay and Sendai MEMS City, Japan, 17-20 April, 2016.
- 26. <u>J. Wenger</u>, Fluorescence enhancement with optical antennas: how to enlarge the reported enhancement without changing the antenna design, Ecole Thématique "Plasmonique Moléculaire et Spectroscopies Exaltées" Toulouse, 20/06/2016
- 27. <u>J. Wenger</u>, Concentrating Light at the Nanoscale, European Summer School on the Physics of Light Strasbourg 07/2015
- 28. <u>J. Wenger</u>, Plasmonic nanoantennas for enhanced single molecule analysis at physiological concentrations, ESF Plasmon-BioNanoSense Barcelona 24/09/2015
- 29. <u>J. Wenger</u>, Plasmonique pour la biophotonique, Workshop Plasmonique : des nouveaux concepts aux applications pratiques, Toulouse, 02/2015
- 30. <u>J. Wenger</u>, Extreme light concentration with plasmonic antennas to enhance fluorescence, Workshop on Extreme light concentration, Paris 06/06/2014
- 31. <u>J. Wenger</u>, Plasmonic nanoantennas for enhanced single molecule analysis at high concentrations, SPIE photonics Europe Nanophotonics V, Brussels 04/2014
- 32. <u>H. Rigneault</u>, 'Nano-Biophotonics: molecular contrast for biomolecular detection and imaging', General seminar Vrije Universiteit Amsterdam, 17 January 2014.
- 33. <u>Deep Punj</u>, Mathieu Mivelle, S. Moparthi, T. Van Zanten, H. Rigneault, N.F. Van Hulst, M. Garcia-Parajo, J. Wenger, Plasmonic nanoantennas for enhanced single molecule analysis at micromolar concentrations, SPP6: the sixth international conference on surface plasmon photonics Ottawa, 2013
- 34. <u>J. Wenger</u>, Plasmonic nanoantennas for enhanced single molecule analysis, Franco-Us workshop on nano-optics, Troyes, 04/11/2013
- 35. <u>J. Wenger</u>, Enhancement and quenching of single emitter luminescence using a dimer gap antenna, MediNano5: 5th Mediterranean conference on nanophotonics Barcelona 05/11/2012
- 36. <u>J. Wenger</u>, Optical antennas to enhance single molecule fluorescence, Second Japan-France Frontiers of Engineering Symposium JFFoE, Kyoto 25/02/2012
- 37. <u>H. Rigneault</u>, 'Optical tools for cell and tissue investigations', Séminaire général de l'Institut Pasteur, 10 Sept 2012, Institut Pasteur, Paris

Dissemination activities targeted to the broad audience (the most relevant ones)

- <u>J. Brugger</u> Rapid prototyping and mass customisation in nanopatterning, Novel nanostructures and their applications Conference and Matchmaking Event. Academia meets Industry: Nanotechnology & High-Energy Physics From Material to Innovation, GSI Darmstadt, Germany, 20-21 October 2016.
- M. F. Garcia-Parajo. "Nanoscale imaging and spectroscopy of living cell membranes using nanophotonic tools". Invited talk at B-DEBATE on *Imaging Life*, Cosmo-Caixa, Barcelona, Spain. 08-09 November 2016.
- N. F. van Hulst, General colloquium: Discussion and Implications on the 2016 Nobel Prize in Chemistry", ICFO Institute of Photonic Sciences, Castelldefels, Barcelona, 17 nov 2016
- R. Regmi (PhD student NANO-VISTA), Journées Scientifiques de l'ED 352, Aix Marseille University, May 2016.
- M. F. Garcia-Parajo. "Acercando la fotónicas a la biologia". Invited seminar ATENEO-EINA, Universidad de Zaragoza, Spain. 16 December 2015.
- N.F. van Hulst Career Session for CIPRIS Fellows QLIMS 2015, Conference on Quantum Light-Matter Interactions in Solid-State Systems, 9-13 November 2015, Barcelona

N.F. van Hulst Conclusion of ESF network - Plasmon-BioNanoSense ESF - Plasmon-BioNanoSense, Concluding Symposium, 24-25 Sep 2015, ICFO - Castelldefels (Barcelona)

<u>N.F. van Hulst</u> ICFO - Light for the Future European Physical Society: IVth Young Minds Leadership Conference, 29-30 May 2015, ICFO Castelldefels (Barcelona)

N.F. van Hulst ICFO - Making Light Work for Society Conferència CERCA - FAPESP, 28-29 May 2015, Barcelona

D. Punj (PhD @NANO-VISTA), Journées Scientifiques de l'ED 352, Aix Marseille, June 2014.

N.F. van Hulst Invited talk, "Antennas for Light: Pushing the fast and the small". Invited traveling lecturer, hbar omega OSA student chapter, Max Planck Institute for the Science of Light. Erlangen. Germany. 18 November 2014.

N.F. van Hulst NFO-school "Session 1: Overview of NanoOptics". NFO-13: 13th international conference of Near-field Optics and Nanophotonics. 31 Aug – 4 Sep 2014, Snowbird, Salt Lake City. United States.

De Torres J., Ghenuche P., Grinenval E., Brennan M., Baffou G., Rigneault H., Wenger J., Nanoantennes plasmoniques pour la biophotonique, Photoniques 65, 37-41 (2013) *journal edited by the French Optical Society SFO*.

CNRS website highlight: Detect a single molecule within a million of others with an optical antenna, http://www.cnrs.fr/insis/recherche/actualites/2013/antennes.htm, retaken as major highlight of the Aix Marseille university for year 2013.

Beyond super-resolution with photonic antennas ICFO website highlight

Antenna-in-box platform to enhance single molecule detection ICFO website highlight

http://www.sciencedaily.com/releases/2013/06/130610095144.htm

http://www.photonics.com/Article.aspx?AID=54128

http://news.silobreaker.com/

http://www.newsbcc.com/australia/science/antenna-in-

box platform for nanoscale biochemical assays with single /476499/

http://www.sciencecodex.com/catching individual molecules in a million with optical antennas inside nanoboxes-113703

http://www.agenciasinc.es/Noticias/Antenas-en-nanocajas-detectan-biomoleculas-individuales

 $\underline{http://www.kurzweilai.net/sensing-individual-biomolecules-with-optical-sensors-inside-nanoboxes}$

http://www.azonano.com/news.aspx?newsID=27573

Connections with other national and European networks

NANO-VISTA has had connections with several national and European networks, where we exchange acknowledge and disseminate the results of the project. We highlight the following events:

- Invited talk of M. F. Garcia-Parajo to the FINON Workshop ITN-EC Female Investigators in non-linear optics. Barcelona, Spain. 26 November 2014.
- Invited talk of N.F. van Hulst to the FINON Workshop ITN-EC Female Investigators in non-linear optics. Barcelona, Spain. 26 November 2014.
- ICFO and CNRS-IF partners are members of the European Erasmus PhD program in Photonics. During NANO-VISTA, we have four PhD students performing joint thesis between Garcia-Parajo (ICFO) & Wenger (CNRS) and van Hulst (ICFO) & Rigneault (CNTS-IF). The topics of the research projects are directly connected to NANO-VISTA.
- Participation of members of NANO-VISTA to the Spanish National CONSOLIDER project "NanoLight" coordinated by N.F. van Hulst (ICFO).

1.5 Address of the project public website & partners contact details:

Public website: www.nanovista.eu

Prof. Maria Garcia-Parajo (coordinator): ICFO-Institute of Photonic Sciences, Barcelona, Spain.

e-mail: maria.garcia-parajo@icfo.es

Prof. Niek van Hulst: ICFO-Institute of Photonic Sciences, Barcelona, Spain.

e-mail: niek.vanHulst@icfo.es

Prof. Juergen Brugger: Institute of Microengineering, EPFL STI IMT LMIS-1, Switzerland

e-mail: juergen.brugger@epfl.ch

Dr. Herve Rigneault: Fresnel Institute, Marseille, France

e-mail: <u>herve.rigneault@fresnel.fr</u>

Dr. Rafael Porcar: COSINGO-Imagine Optic Spain SL, Spain

e-mail: rporcar@cosingo.com

Prof. Alessandra Cambi: Nijmegen Centre for Molecular Life Sciences, the Netherlands

e-mail: A.Cambi@ncmls.ru.nl